Aus der Klinik für Kardiologie
der Medizinischen Fakultät Charité – Universitätsmedizin Berlin

DISSERTATION

FOXO3a and cardiac matrix remodeling- Regulation of MMP-13 expression

zur Erlangung des akademischen Grades
Doctor medicinae (Dr. med.)

vorgelegt der Medizinischen Fakultät
Charité – Universitätsmedizin Berlin

von

Xheni Voloti

aus Durres

Datum der Promotion: 17.09.2021

Table of Contents

ABBREVIATIONS

AdV5 adeno viral vector serotype 5

AFX forkhead box O4 (FOXO4)

Akt cellular homolog of transforming oncogene of Akt-8 oncovirus

AMPK AMP-activated protein kinase

ANP atrial natriuretic peptide

AP-1 activator protein 1 (transcription factor)

ATP adenosine triphosphate

ATS atherosclerosis

BIM Bcl-2-like protein 11

BNIP3 BCL2 interacting protein 3

c-Fos c-Fos-transcription factor

c-Jun c-Jun-transcription factor

C-terminal carboxy-terminal

C. elegans Caenorhabditis elegans

Ca^{2+} calcium

cAMP cyclic adenosine monophosphate

CBP/p300 CREB-binding protein/ E1A binding protein p300

CD16 FcγRIII

cGMP cyclic guanosine monophosphate

CHF chronic heart failure

CK1 casein kinase 1

CMV cytomegalovirus

Cyr61 Cysteine-rich angiogenic inducer 61

D. melanogaster Drosophila melanogaster

DAF-16 orthologous of FOXO in C. elegans

DBD DNA binding domain

DBE Daf-16 family protein-binding element

DCM dilated cardiomyopathy

DNA Deoxyribonucleic acid

E3RS1kB/ β-TrCP SCF-type E3 ubiquitin ligase

ECM extracellular matrix

EMMPRIN extracellular metalloproteinase inducer

ERK	extracellular-signal-regulated kinase
ETS	E26 transformation-specific or E-twenty-six
FGF	fibroblast growth factor
FKHR	FOXO1
FKHRL-1	forkhead box O3a
FOX	forkhead box
FOXA3	hepatocyte nuclear factor 3-gamma
FOXO	forkhead box O
FOXO3a-/-	FOXO3a *knockout*
FOXO3a+/+	FOXO3a *wildtype*
Gadd45	growth Arrest and DNA Damage-inducible 45
GFP	green fluorescent protein
GSK3ß	glycogen synthase kinase 3ß
GTPase Ral	Ral guanosine triphosphatase
H_2O	water
HPRT1	hypoxanthine phosphoribosyltransferase 1
HUVECs	human umbilical vein endothelial cells
IGF-1	insulin-growth factor-1
IKK	IκB kinase
IL-1β	interleukin-1β
IL-6	interleukin-6
IRE	insulin-response element
JNK	c-Jun N-terminal kinase
KO	knock out
LMTK3	Lemur Tyrosine Kinase 3
LV	left ventricle
LY294002	selective PI3k inhibitor
MAPK	mitogen-activated protein kinase
MCP-3	monocyte chemotactic protein-3
MI	myocardial infarction
MMP	matrix metalloproteinase
MnSOD	manganese superoxide dismutase
MOI	multiplicity of infection

MST-1	macrophage-stimulating protein 1
MT1-MMP	membrane type- 1 matrix metalloprotease
mTOR	mammalian target of rapamycin
Murf-1	ubiquitin-ligase
NES	nuclear export sequence
NF-kB	nuclear factor 'kappa-light-chain-enhancer' of activated B-cells
NH_2-	amino-terminal
NK cell	natural killer cell
NLS	nuclear localization sequence
NRFB	neonatal rat fibroblast
NRVM	neonatal rat ventricular myocyte
$p21^{CIP1}$	CDK-interacting protein 1
p27	cyclin-dependent kinase inhibitor 1B
p38	a class of MAPK
PDGF	platelet derived growth factor
PEA-3	polyomavirus enhancer activator 3 (transcription factor)
PI3k	phosphatidylinositol 3-kinase
PKB	protein kinase B
PTM	post-transcriptional modification
qRT-PCR	quantitative real time polymerase chain reaction
RanGTPase	Ras-related Nuclear protein guanosine triphosphatase
ROS	reactive oxygen species
SCF	Skp1, Cullins, F-box proteins
SGK	serine/threonine-protein kinases
siRNA	small interfering RNA
SIRT	sirtuin (silent mating type information regulation 2 homolog)
SNP	single-nucleotide polymorphism
TA	transactivating domain
TGF-ß	transforming growth factor ß
Thr32	threonin 32
TIE	TGF-ß inhibitory element
TIMP	tissue inhibitor of metalloproteinase
TM-FOXO3a	triple-mutant FOXO3a
TNF-α	tumor necrosis factor α

VEGF	vascular endothelial growth factor
VSMCs	vascular smooth muscle cells
Zn	Zinc

Abstrakt

Hintergrund: Das kardiale Remodeling spielt bei vielen kardialen Erkrankungen, wie beispielsweise einer Volumenüberlastung (Mitralinsuffizienz), einer Drucküberlastung (Aortenstenose, Hypertonie), einer Entzündung (Myokarditis), genetischen Erkrankungen (DKM) oder einer Ischämie (Myokardinfarkt) eine bedeutende Rolle. Die Charakterisierung von Signaltransduktionswegen im kardialen Remodeling wird derzeitig aktiv untersucht. MMPs sind Endoproteinasen, die den Umsatz der extrazellulären Matrix (EZM) beeinflussen, und ihre Rolle wurde mit dem Remodeling in Verbindung gebracht. MMP-13 ist eine Kollagenase, die im gesunden Myokard in sehr niedrigen Konzentrationen exprimiert wird, aber im Remodeling-Prozess hochreguliert ist. FOXO3a ist ein Transkriptionsfaktor, der eine wichtige Rolle bei verschiedenen grundlegenden biologischen Prozessen wie der Entgiftung von toxischen Sauerstoffradikalen, dem Glukosestoffwechsel, der DNA-Reparatur, dem Zelltod und der adaptiven Zellgrösse von kardialen Myozyten spielt. Seine Rolle beim kardialen Remodeling der extrazellulären Matrix wurde bisher noch nicht untersucht.

Methodik: Neonatale kardiale Rattenfibroblasten (NRFB) und Kardiomyozyten (NRVM) wurden in vitro mit einem replikationsdefekten adenoviralen Kontrollvektor (AdV5-CMV-GFP) oder einem adenoviralen Vektor, der konstitutiv aktives FOXO3a (ADV5-CMV-TM-FOXO3a) oder WT-FOXO3a kodiert, transduziert. Die mRNA Expression verschiedener EZM- Regulatoren wurde mittels qRT-PCR quantifiziert. Die Proteinexpression sowie die Siagnaltransduktion wurde mittels Western blotting charakterisiert. DNA- Bindungsassays und Promoteranalysen dienten der Aufklärung der mechanistischen Effekte von FOXO3a. Funktionell wurde die Kollagenase-Aktivität bestimmt. Diese Ergebnisse wurden auch mit Hilfe von FOXO3a defizienten Mausfibroblasten bestätigt. Die *in vivo* Effekte von FOXO3a wurden in einem murinen Infarktmodell sowie Myokarditismodell determiniert.

Ergebnisse: Die Transduktion der NRVM mit WT-FOXO3a oder TM-FOXO3a zeigte keine Hochregulation von MMP-1, -3, -9, TIMP-1, -2 und -4. Die Überexpression von FOXO3a in NRFB und NRVM resultierten in einer dosisabhängigen Erhöhung der MMP-13 mRNA. Darüber hinaus führte endogenes FOXO3a zu einer höheren Expression von MMP-13 mRNA in beiden Zelltypen. Durch das Kollagenase-Assay wurde auch eine erhöhte kollagenolytische Aktivität in NRFB nach FOXO3a Überexpression nachgewiesen. In dem Infarktmodell führte die Aktivierung von

FOXO3a zu einer Hochregulation von MMP-13. FOXO3a-/- Mäuse zeigten eine Hochregulation von MMP-13 in einem viralen Myokarditismodell.
Schlussfolgerung: FOXO3a führt über die Hochregulation der MMP-13 Expression zum Kollagen-Abbau. Der Transkriptionsfaktor spielt eine bedeutende Rolle in der Koordination von Zellgrösse und Remodeling der extrazellulären Matrix. Weitere Studien der FOXO3a Effekte auf die Zell-Matrix-Interaktion in kardialen Schädigungsmodellen können einen eventuellen klinischen Nutzen dieser Interaktion definieren.

Schlüsselwörter: kardiales Remodeling, FOXO3a, MMP-13, kardialer Fibroblast, Kardiomyozyt

Abstract

Background: Cardiac remodeling plays an important role in cardiac disease such as volume overload (mitral regurgitation), pressure overload (aortic stenosis, hypertension), inflammation (myocarditis), genetical disorders (DCM) or ischemia (myocardial infarction). The characterization of signaling pathways in cardiac remodeling is still under investigation. MMPs are endoproteases that influence ECM turnover and their role has been implicated in remodeling. MMP-13 is a metalloprotease expressed at very low levels in the healthy myocardium, but it is up-regulated in the remodeling process. FOXO3a is a transcription factor that plays an important role in diverse basic biological mechanisms such as detoxification of toxic oxygen derived radicals, glucose metabolism, DNA-repair, apoptosis and adaptive cardiac myocyte size. However, its role in cardiac matrix remodeling has not as yet been studied .

Methods: Neonatal rat cardiac fibroblasts (NRFB) and cardiomyocytes (NRVM) were transduced in vitro with a replication defective adenoviral vector (AdV5-CMV-GFP) or an adenoviral vector that encodes a constitutively active FOXO3a (AdV5-CMV-TM-FOXO3a) or wild-type FOXO3a (WT-FOXO3a). mRNA expression of various ECM regulators was quantified by qRT-PCR. Protein expression and signal transduction pathways were characterized using western blotting. DNA-binding assays were used to better understand the mechanistic effect of FOXO3a. On a functional level, the collagenolytic activity was determined. The results were also confirmed *in vivo* using FOXO3a deficient mouse fibroblasts. Effects of FOXO3a were determined in a murine MI and viral myocarditis model.

Results: Transduction of NRVM with WT-FOXO3a or TM-FOXO3a did not change expression levels of MMP-1, -3, -9 or TIMP-1, -2 or -4. However, TM-FOXO3a gene transfer dose-dependently up-regulated MMP-13 mRNA and protein expression. Furthermore, endogenous FOXO3a led to higher levels of MMP-13 mRNA in both cell types. An increased collagenolytic activity was detected in NRFB after FOXO3a overexpression by collagenase assay. Mechanistically, FOXO3a directly binds and trans-activates the MMP-13 promoter in NRVM. The up-regulation of MMP-13 could also be confirmed in *in vivo* models of cardiac injury i.e. MI in FOXO3a *wildtype* and *knockout* mice. Moreover, FOXO3a-/- showed an up-regulation of MMP-13 mRNA levels in the CVB3 murine myocarditis model.

Conclusions: Transduction of NRVM with WT-FOXO3a or TM-FOXO3a did not influence the expression of MMP-1, -3, -9 or TIMP-1, -2 or -4. Through up-regulation of MMP-13 expression, FOXO3a leads to collagen degradation. The transcription factor plays an important role in the coordination of cell size and cardiac matrix remodeling. Further studies of the effect of FOXO3a on cell-matrix interaction in cardiac injury models would define a potential clinical use of this interaction.

Keywords: cardiac remodeling, FOXO3a, MMP-13, cardiac fibroblast, cardiomyocyte

INTRODUCTION

Within the healthy myocardium, the permanent set of cells is composed of cardiomyocytes, cardiac fibroblasts, endothelial cells and vascular smooth muscle cells. The non-permanent group consists of immune cells such as lymphocytes, mast cells, monocytes and macrophages. These transient cells move towards the myocardium from the vascular compartment in the case of pathological conditions and cooperate with the permanent set of cells to restore cardiac function (1).
The cardiomyocyte is the main and sole contractile unit of the heart. As this cell is largely incapable of replication, its survival is crucial. As such pivotal an element of the cardiac function, it is provided with a very complex and well-structured endorsement system of cells and molecules, the cardiac extracellular matrix (ECM), that provides bio-mechanical support designated to preserving its structural and functional integrity.
The cardiac extracellular matrix encapsulates all cells, structural proteins and bio-active molecules creating a unique auxiliary system to the homeostasis of the cardiomyocyte. Initially, it was Steeter and Bresset who investigated the importance of the complex architectural arrangement of the cardiac extracellular matrix in preserving the cardiomyocyte orientation and therefore assuring its correct functioning (2). These authors demonstrated that the orientation of the cardiomyocytes along with the myocardial fiber angles were highly organized and directed from the endocardium towards the epicardium (2). This research group was the first to provide insight on the importance of a homeostatic ECM in regards to cardiomyocyte's physiological functionality.

Cardiac remodeling

The plasticity of the heart potentiates ventricular remodeling following physiological and pathological stimuli. Early phase, adaptive, and late phase, maladaptive, remodeling patterns can be recognized in almost every model of cardiac pathology including volume (mitral regurgitation) or pressure overload (aortic stenosis, hypertension), inflammation (myocarditis), genetic disorders (DCM) and ischemia (myocardial infarction) (3).

Hochman and Bulkley were the first to observe regional dilation and thinning of the infarcted area (4). Subsequently, Pfeffer et al. used the term remodeling to describe the volume increase of the left ventricular cavity following myocardial infarction (MI) (5). According to the Consensus Paper of the International Forum on Cardiac Remodeling, "… cardiac remodeling may be defined as genome expression, molecular, cellular and interstitial changes that are manifested clinically as changes in size, shape and function of the heart after cardiac injury " […] "The process of cardiac remodeling is influenced by hemodynamic load, neuro-hormonal activation and other factors still under investigation. The myocyte is the major cardiac cell involved in the remodeling. Other components involved in this complex process include fibroblasts, the interstitium, collagen and the coronary vasculature; relevant processes also include ischemia, cell necrosis and apoptosis" (6).

Grossman's systolic and diastolic- stress- correction hypothesis, respectively on pressure and volume overload induced wall stress, depict the early stage compensatory hypertrophy of the myocytes aimed to lower the wall stress and maintain cardiac function (7). Relying on the Laplace law, pressure overload can cause an increase in cardiomyocyte width resulting in increased wall thickness, what Grossman defined as concentric hypertrophy, where newly formed sarcomeres are disposed in parallel. Increased diastolic wall stress due to volume overload, gives rise to cardiomyocyte elongation with eccentric hypertrophy, resulting in increased ventricular diameter (newly formed sarcomeres are disposed in series). However, extensive studies have questioned the classic wall-stress hypothesis and recent research has put an emphasis on the nature of the initial signaling stimulus (8).

The typology of the growth stimulus determines whether the cardiomyocyte survives or undergoes apoptosis. Growth stimuli that promote myocyte survival, are recognized as stimuli of beneficial hypertrophy. In contrast, mechanistic pathways that promote apoptosis cause left ventricular dysfunction (9) (10). Thus, different molecular signal transduction pathways, result in either adaptive or maladaptive patterns of hypertrophy. Adaptive mechanisms of myocyte growth are considered those resulting from the activation of IGF-1 and atrial natriuretic peptide (ANP) pathways. IGF-1 stimulates the activation of Akt, a serine-threonine kinase which strongly promotes cellular growth by phosphorylating GSK3ß (inhibition), FOXO3a (inhibition), mTOR (activation) and p70 kinase (activation). The production of cyclic guanosine monophosphate (cGMP) in response to ANP restricts hypertrophy. These signaling pathways promote growth and

inhibit cell death (8). Consequently, remodeling resulting from these stimuli, favors the restoration of a physiological left ventricular function.

Maladaptive patterns of pathological left ventricular remodeling include those cellular pathways that promote cell death (angiotensin II through MAPK pathways), fibrosis (TGF-ß, aldosterone) and extracellular matrix degradation (ECM) (MMP/TIMP imbalance, favoring MMPs activity with subsequent deposition of incorrectly cross-linked collagen and myocyte 'slippage') (8).

All of the above maladaptive patterns involve either quantitative or qualitative modifications of the collagen fibers of the ECM.

Myocardial collagen type I and III are regarded as important proteins of the cardiac ECM. These proteins safeguard the integrity of contiguous cardiomyocytes. Additionally, they maintain the alignment of the myofibrils through a collagen-integrin-cytoskeletal myofibril axis (11).

Woodiwiss et al. investigated the impact of collagen cross-linking on the left ventricular function. The research group found that anomalies in collagen cross-linking correlated with left ventricular dilation (12). Furthermore, Weber et al. analyzed postmortem specimens from patients with idiopathic dilatative cardiomyopathy. Compared to samples from healthy individuals, myocardium samples from patients with idiopathic dilatative cardiomyopathy presented incorrect collagen tethering (13).

Collagen is subject to degradation by metalloproteinases, which, along with their inhibitors (TIMPs), have also been implicated in the pathogenesis of various cardiac diseases.

An MMP/TIMP imbalance, favoring MMP activity, concomitant with the activation of the plasminogen system and the increase in cytokine levels, correlates with left ventricular dysfunction in myocarditis. The MMP/TIMP imbalance disrupts the homogeneity and integrity of a homeostatic ECM, perpetuating this effect onto the global worsening of the left ventricular function (14).

Important contributors to the maladaptive patterns of cardiac remodeling are also the following mechanisms: increased production of reactive oxygen species (ROS) (increased fibrosis and myocyte death), energy and metabolism alterations (decreased ß-oxidation leading to lipotoxicity and ROS formation), modifications of levels of intracellular Ca^{2+} (ROS formation and mitochondrial fragmentation with subsequent apoptosis) and contractile proteins leading to altered contractile function (15).

FOXO3a and MMP-13 are proteins implicated in processes similar to those occurring in cardiac remodeling such as apoptosis, cardiac cell size, ECM degradation and ROS metabolism.

Forkhead box (FOX) class of transcription factors

The Forkhead box (FOX) class of transcription factors are a conserved evolutionary group of proteins firstly identified in 1989 by Weigel and Jäckle (16). Initially, they were identified as proteins involved in the embryonic development of D. melanogaster. Weigel and Jäckle named the gene DAF-16. The most characteristic feature of the FOX proteins is the forkhead box, known also as the winged helix. This is the portion of the protein which binds the DNA. These proteins have been identified in different species from yeast to human (17).

The FOX gene in mammals is the orthologue of the DAF-16 gene in the D. melanogaster. This family of transcription factors includes at least 100 proteins categorized into 17 subgroups identified as A-Q (18).

The “O” subgroup comprises four members in mammals: FOXO1 (also known as FKHR), FOXO3a (also known as FKHRL1), FOXO4 (also known as AFX) and FOXO6. FOXO3a is the most represented FOXO protein in the myocardium (19).

They are transcription factors that are involved in different cellular functions such as: stress resistance, cell cycle arrest, control of metabolism, apoptosis, tumor cell suppression, DNA repair, autophagy, proteolysis, longevity, differentiation and development (20) (21).

Each FOXO protein has four domains: the DNA-binding domain (DBD), the nuclear localization sequence (NLS), the nuclear export sequence (NES) and the transactivating domain (TA). DBD, NLS and TA are the most conserved sequences amongst the FOXO proteins (20).

DNA recognition and interaction

Structure of the DBD

The first study to investigate the FOX protein-DNA interaction was performed by Clark et al. (22). This study focused on the interaction between the DBD of the FOXA3 and

DNA. FOXA3, also known as hepatic nuclear factor 3 gamma, is exclusively expressed in the liver. This forkhead transcription factor is involved in cell differentiation and glucose homeostasis (23). Clark and colleagues came to the conclusion that the forkhead/winged helix domain contains about 100 amino acids that are organized into three α-helices (H1, H2 and H3), three ß-helices (S1, S2 and S3) and two wing-like hoops known as W1 and W2. These residues are arranged in the following order: H1-S1-H2-H3-S2-W1-S3-W2. The NH_2-terminal of FOXO3a is formed by the three α-helices. S1 is situated between H1 and H2. A three stranded, twisted, anti-parallel ß -sheet formed by S2 and S3 faces the DNA (20).

There are two conserved sequences recognized by all FOXO proteins: the 5'-GTAAA(T/C)AA-3' sequence, known as the DAF-16 family member binding element (DBE), and the 5'-(C/A)(A/C)AAA(C/T)AA-3' sequence, known as the insulin-response element (IRE) (20). Both sequences include the core sequence 5'-(A/C)AA(C/T)A-3' recognized by all forkhead proteins (20). FOXO proteins can bind both sequences, but they have a higher affinity for the DBE (20). The H3 helix is in contact with the major groove of the DNA and it represents the predominant and most extensive contact site of FOXO3a with DNA (20). Asn165 and His169 are highly conserved in all forkhead proteins (20). Contacts between DBD and DNA involve direct hydrogen bonds between side chains and bases, water-mediated side chain-base interactions and van der Waals contacts with both bases and the backbone of the DNA (20).

Although interaction with the DNA might be similar between FOXO proteins, recognition patterns may be different. Variability regions include the NH_2-terminal sequence preceding helix H1, the region between helices H2 and H3, wing W1 and the C-terminal segment. These regions provide control of the DNA-binding affinity and the stability of the forkhead DBD-DNA complex (20).

FOXO3a interaction with DNA

Similar to other FOXO proteins, the H3 helix is crucial for the recognition of the core sequence (20). Tsai et al. have specifically studied the interaction between the FOXO3a DBD and DNA (24). According to their findings, "the DNA recognition specificity of FOXO3a is due to a series of van der Waals contacts between the methyl groups of the thymine bases and the side chains of Arg211, Ser215 and His212 within the recognition helix. W1 and the C-terminal contribute to DNA binding. The C-terminal of FOXO3a-

DBD, which functions as NLS and contains a PKB phosphorylation site and 14-3-3 binding motif, adopts a coil structure inserted into the major groove of DNA. Hence, the C-terminal region of FOXO3a-DBD plays a crucial role in stabilizing the formation of the complex with DNA" (24).

Regulation of FOXO3a activity

FOXO3a target gene expression is typically under the control of stimuli from growth factors or cellular stress conditions such as fasting or oxidative stress (21). FOXO3a regulation affects the activity as a transcription factor, influencing its subcellular localization and DNA affinity, and its levels as a protein, through protein degradation, transcription levels and FOXO3a gene mutation. The fastest and most versatile modifications of FOXO3a activity are achieved through post transcriptional modifications, known also as PTMs: phosphorylation, acetylation and ubiquitination. Influences on FOXO3a protein levels translate into more long-term effects on cellular function. This to the extent that, several studies report a loss of FOXO3a to be associated with tumorigenesis (21).

FOXO3a activity modulation: subcellular localization and DNA affinity

Phosphorylation of FOXO3a

FOXO3a can target specific gene expression when localized in the nucleus. Nucleo-cytoplasmic shuttling of FOXO3a inhibits its activity and stores FOXO3a in the cytoplasm in an inactive form (25). Akt, SGK, ERK, CK-1 and IKK are protein kinases that can phosphorylate FOXO3a at specific sites and enable its nuclear export having an inhibitory effect on the transcriptional activity of FOXO3a (26). FOXO3a is also subject to phosphorylations that promote its role as a transcription factor. Upstream regulators of FOXO3a such as JNK, AMPK, MST1 and LMTK3 can directly or indirectly influence the nuclear import of FOXO3a with consequent implementation of its function as a transcription factor (26).

Nuclear export of FOXO3a

In the presence of growth factors, PI3k activates Akt, which in turn phosphorylates FOXO3a and promotes its nuclear export (25). Initially, Akt phosphorylates FOXO3a at Thr32 and Ser253 (25). These phosphorylation sites create binding sites for the 14-3-3 proteins facilitating the consequent FOXO3a nuclear export (25). In addition, the Akt phosphorylation on Ser315 is required for CK1 phosphorylation of Ser318 and Ser321 (26). These phospholyrations allow FOXO3a to interact with RanGTPase, a component of the exportin/Crm-1 export machinery that leads to the nuclear export of FOXO3a (27). Akt phopsphorylation sites disrupt NLS activity facilitating binding of the 14-3-3 proteins that probably mask the NLS and expose the NES (28) and consequent association with the nuclear export machinery (27). SGK can also phosphorylate FOXO3a at the Akt phosphorylation sites, though with different site preference than Akt: both phosphorylate the Thr32 site equally well, however, SGK shows a preference for the Ser315 site and Akt for the Ser253 site (29). Furthermore, ERKs have been demonstrated to inhibit FOXO3a by directly phosphorylating FOXO3a at Ser294, Ser344 and Ser425, and to induce the degradation of FOXO3a via the murine double minute-2 signaling pathway (26). IKK, a downstream target of the TNF-α signaling pathway, can phosphorylate FOXO3a at Ser644, promoting cytoplasmic retention and polyubiquitination-mediated degradation of FOXO3a (26).

Nuclear import of FOXO3a

The nuclear import of FOXO3a takes place under cellular stress conditions. Oxidative stress activates GTPase Ral, which in turn activates JNK (30). JNK can phosphorylate FOXO3a at Ser574, which antagonizes the Akt signaling pathway and promotes the transcription and nuclear translocation of FOXO3a (26). AMPK can phosphorylate FOXO3a at six different sites (Ser399, Thr179, Ser413, Ser588, Ser555 and Ser626), causing an increase in the activity of FOXO3a without affecting its subcellular localization (31). Furthermore, MST1 (mammalian Ste20-like kinase) phosphorylates FOXO3a at Ser207. MST1 phosphorylation of FOXO3a disrupts 14-3-3 binding, thereby triggering the relocalisation of FOXO3a from the cytoplasm to the nucleus (21). LMTK3 (lemur tyrosine kinase-3) is a serine-threonine-tyrosine kinase that can inhibit protein kinase C and Akt, thereby promoting the binding of FOXO3a to the estrogen receptor 1 gene promoter element (26).

Acetylation/deacetylation of FOXO3a

CBP/p300 mediates FOXO3a acetylation. It can acetylate nucleosomal histones and stimulate transcription of the acetylated DNA fragment. At the same time, FOXO3a is also acetylated, but its activity was found to be decreased by such modification in a study by van der Heide and colleagues (32).
Different studies have shown a controversial influence of Sirt1-mediated deacetylation of FOXO3a. Motta et al. were the first to show an inhibitory effect of Sirt1 deacetylation on the FOXO3a transcriptional activity (33). Interestingly, Brunet et al. have reported that Sirt1 has a dual effect on the FOXO3a function (34). Sirt1, through up-regulation of FOXO3a transcriptional activity, increases the expression of p27 and Gadd45, genes involved in cell cycle arrest and DNA repair. On the other hand, the same study showed a decrease in pro apoptotic BIM levels (34). In addition to Sirt1, other sirtuins such as Sirt2 and Sirt3 are involved in the regulation of the FOXO3a DNA-binding activity (26). Sirt2 increases the binding of FOXO3a to the p27 promoter region (26). Sirt3 is a mitochondrial sirtuin that enhances FOXO3a up-regulation of MnSOD (manganese superoxide dismutase), an enzyme involved in the detoxification of ROS (26).

Ubiquitination of FOXO3a

IKK (IkB kinase) is a down-stream target of the TNF-α signaling pathway. Proteasome-mediated degradation of FOXO3a through polyubiquitination results from IKK phosphorylation at Ser644 (35). A phosphorylated IκB serves as an essential part of a specific recognition site for E3RSIκB/β-TrCP, an SCF-type E3 ubiquitin ligase, (36)

FOXO3a protein levels

Degradation of FOXO3a in a proteasomemanner follows phosphorylation by IKK, in response to TNF-α stimulation (35).
Rearrangements at the FOXO3a gene loci can also lead to modification of FOXO3a protein levels in the cell. FOXO3a genes are present at chromosomal translocation break points in cells of acute myeloid leukemias. These chromosomal translocations

result in chimeric transcription factors where the transactivation domain is fused to the DNA-binding domain of other transcription factors (21).

FOXO3a and cardiac remodeling

The role of FOXO3a in cardiac remodeling has been attributed to its ability to induce atrophy related genes. Skurk et al. have shown that the activation of FOXO3a in cardiac myocytes inhibits hypertrophy in vitro (Figure 1) (37). Furthermore, FOXO3a-gene transfer led to reduction in cardiomyocyte size in mouse hearts *in vivo* (37). FOXO3a and FOXO1 exerted atrophic effects in skeletal muscle (38) (39). As cardiac hypertrophy is a major element characterizing cardiac remodeling, the ability of FOXO3a to induce atrophy is positively correlated with the amelioration of cardiac remodeling.

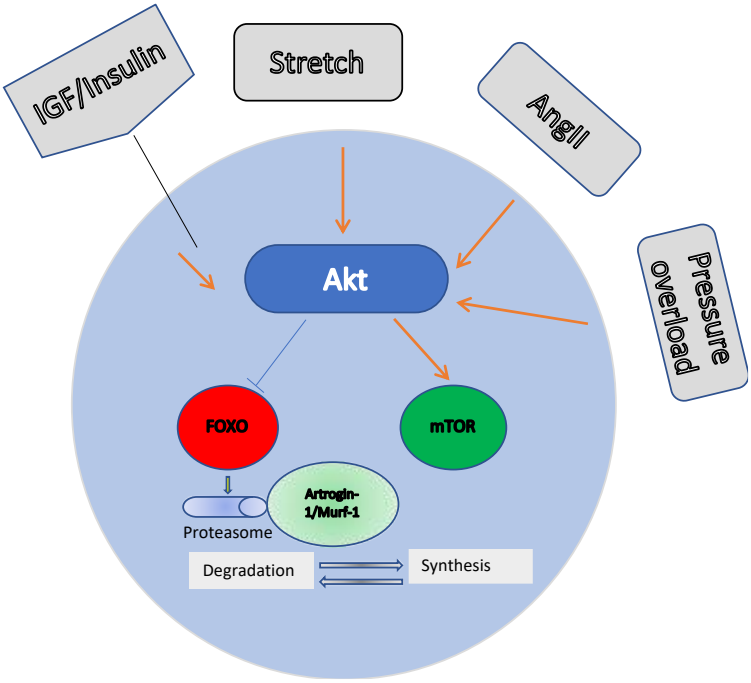

Figure 1: Illustration for Akt/FOXO-mediated regulation of cardiac myocyte size. Akt can be phosphorylated and activated by different growth stimuli (angiotensin II, IGF, insulin) and mechanic stimulation (stretch, pressure overload). Akt induces cardiomyocyte hypertrophy by up-regulating protein synthesis through the mammalian target of rapamycin-dependent pathways. Akt activation inhibits FOXOs through phosphorylation. FOXO transcription factors activate atrogenes, including the ubiquitin ligases atrogin-1 and MuRF-1, which promote proteolysis (Modified according to Skurk et al. (37).)

Metalloproteinases (MMPs)

The cardiac fibroblast is the key cell that synthesizes and organizes the ECM, which has been subject to extensive research in the past decades. What we once thought to be a static structure is in fact a dynamic and complex bioactive support system. A homeostatic cardiac ECM not only confers stability and plasticity to the tissue, it is also a reservoir of bioactive molecules such as growth factors and cytokines intercalated between cells.

There are two main classes of proteins that constitute the cardiac ECM: a) fibrous and adhesion proteins and b) glycoproteins (non-fibrillar proteins). The first group includes proteins such as collagen, fibronectin, laminin and elastin. Not only do they confer structural stability and elasticity to the tissue, they also provide adhesion sites for the surrounding cells. This fibrillar matrix facilitates the effective transmission and absorption of cyclical tensile forces while avoiding injury (40).

Non-fibrillar proteins are extensively glycated glycoproteins. They are negatively charged, which enables them to covalently bind molecules of H_2O to keep the ECM and the cells hydrated.

Collagen is the most important structural protein of the ECM that confers stability to the tissue. There are 28 types of different collagens and each is organized in either homotrimers or heterotrimers formed by three polypeptide chains, known as alpha-chains. The triple helix of these α chains is the structural hallmark of fibrillar collagen. More than 40 types of α chains have been discovered (41).

Myocardial fibrillar collagen is distributed and arranged into three layers: the epimysium, the perimysium and the endomysium. The epimysium is the most upper layer of fibrillar collagen that folds the myocardium. The collagen fibers ramify to surround groups of cells forming the perimysium. The endomysium is an individual myocyte layer of collagen that also connects the cell to the capillaries. (15) (42).

The ECM protein content degradation is specifically targeted by a group of endopeptidases known as matrix metalloproteases. They are Zn-dependent proteases and at least 25 types have been identified in human cells (2). Many classes of MMPs have been identified in the mammalian myocardium such as collagenases and gelatinases as listed in Table 1 (2). They are synthesized as inactive zymogens and secreted as pro-peptides. They reside in the ECM as latent, inactive enzymes until activation. Each MMP contains four major domains: the catalytic domain, containing the

binding site for the Zn atom, the pro-peptide, where the single cysteine residue is present, the signal peptide and the hemopexin/vimentin domain, which is not present in MMP-7 (2).

Table 1: Representative MMP classes and their members identified in the mammalian myocardium.

Name		**Taxonomy number**	**Substrate**
Collagenase	Interstitial collagenase	MMP-1	Collagens I, II, III, IV, and basement membrane components
	Collagenase 3	MMP-13	Collagens I, II, III,
	Neutrophile collagenase	MMP-8	Collagens I, II, III, gelatins
Gelatinase	Gelatinase A	MMP-2	Gelatins, collagens I, IV, V, VII, and basement membrane components
	Gelatinase B	MMP-9	Gelatins, collagens IV, V, XIV, and basement membrane components
Stromyelisin	Stromyelisin 1	MMP-3	Fibronectin, laminin, collagens III, IV, IX, and MMP activation
	Matrilysin	MMP-7	Fibronectin, gelatins, and basement membrane components
Membrane-type MMP	MT1-MMP	MMP-14	Collagens I, II, III, fibronectin, laminin-1; activates pro-MMP-2 and pro-MMP13

The most recognized mechanism of MMP activation is the “cysteine switch”. The single cysteine present in the pro-peptide domain, binds the Zn atom and blocks the active site. The cleavage of the cysteine, dissociating it from the Zn atom, leads to exposure of the active site of the MMP. Activation of MMPs therefore is associated with a decrease in molecular weight, due to the release of the amino group of the cysteine (2).

AP-1 and PEA-3 binding sites are the most conserved binding site in the promoter region of MMPs. AP-1 transcription factors (c-Jun and c-Fos) are part of the signaling

pathway initiated by growth factors or cytokines. Cell differentiation and cell cycle is one of the many functions of the ETS family of transcription factors which binds to the PEA-3 binding element (2). Specifically, MMP-13 contains a TGF-ß inhibitory element (TIE) as well an NF-kB binding site (2). Most importantly, the MMP-13 promoter contains conserved binding sequences for FOXO3a in different species as illustrated in Figure 2 (43).

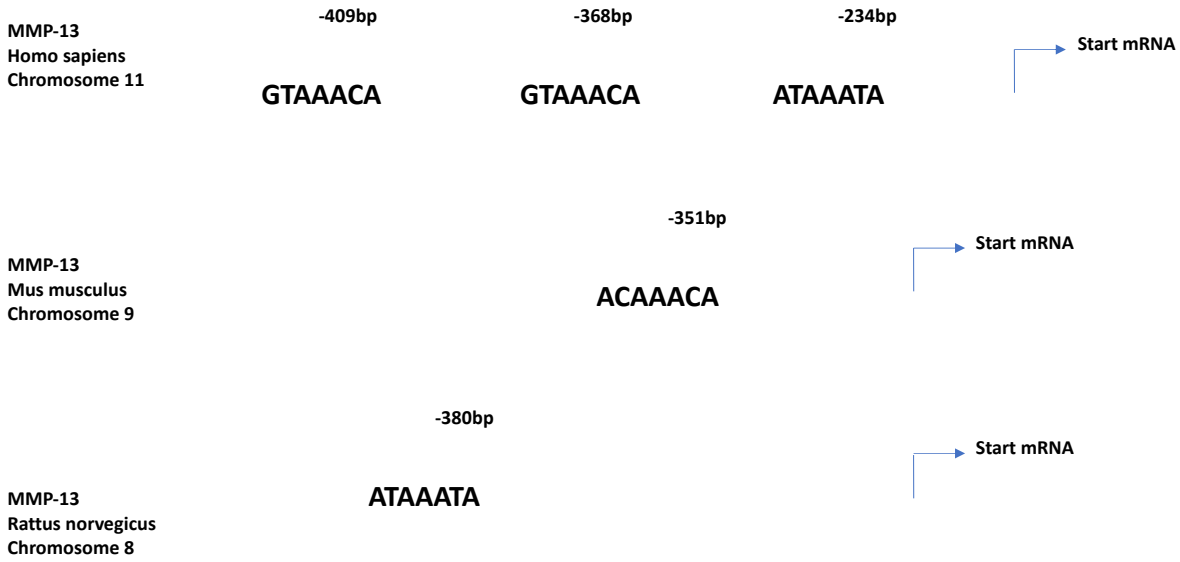

Figure 2: Representation of the MMP-13 promoter region in different species. MMP-13 promoter proximal site contains the core sequence recognized by FOXO3a. (Modified according to Yu et al. (43))

There is an intricate system of stimuli and molecules that can activate and control the activity of MMPs. Transcriptional and post-transcriptional modifications control the activity of MMPs. Transcriptional factors that can activate binding elements in the promoter region of the MMPs influence gene expression. Post-transcriptional modifications include splicing and activation or activation/inhibition of MMP activity. EMMPRIN is a recognized MMP activator, whilst TIMPs have an inhibitory effect on MMP activity. TIMPs bind to the catalytic domain of MMPs, thus making it inaccessible to the substrate [2].

MMPs are essential for ECM turnover and tissue remodeling. They have been implicated in different processes such as reproduction, wound healing and bone growth (2). MMPs are involved in a plethora of processes such as cell migration, differentiation, tissue organization and ECM degradation. According to *in vivo* and *in vitro* studies, MMPs have been associated with important developmental and physiological

processes. During the development of the placenta, invading trophoblasts express high levels of MMP-9 (44). MMPs are also important in bone development (MMP-9, MMP-14, MMP-13) (45), development of the nervous system (MMP-9) (46), keratinocyte migration (MMP-1) and fibroblast contraction (MMP-3) during wound healing (47). They have also been identified to have a biological significance in pathological conditions such as cancer, inflammatory disease and cardiovascular disorders. Increased expression of MMPs by cancerous cells is associated with tumor invasion and adds to its metastatic potential.

MMPs have substrate affinity for different types of ECM molecules resulting in their activation, inactivation, release of active or inactive fragments or increased bioavailability. Such modifications of the extracellular environment provide different stimuli that lead to the activation of many intracellular-signaling pathways resulting in different cellular responses. MMP-3, -7, -9, -12 can cleave plasminogen and generate angiostatin, an anti-angiogenic molecule. Cleavage of collagen XVIII with release of endostatin and cleavage of antithrombin III also results in the release of anti-angiogenic fragments (47).

MMP-2, -3 and -7 can release TGF-ß bound to decorin (48). MMP-1 and MMP-3 can degrade perlecan and release FGF (49). MMP-13 releases biologically active soluble TNF-α from its membrane bound precursor form (50).

MMP-2, -3, and -9 can process the precursor of IL-1ß to release an active form of it (51). MMP-2 can cleave endothelin-1 into a more powerful vasoconstrictor. (52). MMP-8 can transform angiotensin I to angiotensin II through cleavage (53). MMP-13 cleaves and inactivates the monocyte chemoattractant protein (MCP) -3 (54).

MMP-13

MMP-13 degrades most of the structural and non-structural proteins of the ECM. It has a high substrate specificity for collagen I and III but it also cleaves collagen IV, IX, X, XIV, aggrecan, perlican, versican, gelatin and proteoglycans (2) (55).

Since it can cleave different types of ECM constituents, its expression has been associated with different types of cancers. MMP-13 expression has been shown in esophageal carcinoma (56), basal cell carcinoma (57), chondrosarcoma (58), melanoma (59) and vulvar squamous cell carcinoma (60).

MMP-13 is also expressed and up-regulated in diseases with a characteristic pattern of chronic inflammation such as: atherosclerosis [48], intestinal ulcerations (61), osteoarthritis (62) and rheumatoid arthritis (63). Within the normal myocardium MMP-13 is only expressed at very low levels but is up-regulated in end-stage congestive heart failure (64). Spinale et al. were the first to describe the role of MMP-13 in dilated cardiomyopathy as the predominant interstitial collagenase (64). MMP-1 and MMP-13 do cleave fibrillar collagens I and III (65). The observed reduction of MMP-1 levels in DCM combined with an increase in MMP-13 leads to a persistent interstitial collagenolytic activity within the myocardium (64). Thus, spatially and timely propagating left ventricular remodeling, phenotypically progressing towards dilation of the left ventricle.

MMP-13 is activated by MT1-MMP, but MMP-1 is not (64) (66). MT1-MMP does cleave fibrillar collagen (64) (67). With MMP-1 not being activated by MT1-MMP there is an increased susceptibility of the failing human myocardium to fibrillar collagen degradation.

IL-1ß and IL-6 are known to be increased within 24 hours after myocardial infarction (MI), leading the chemotaxis of immune cells to reach the site of injury. Both of these cytokines induce the expression of MMP-13. The induction by IL-1ß, in the presence of TNF-α, requires p38, JNK and NF-kB, which interact with the AP-1 region of the MMP-13 promoter, increasing its activity (68) (69).

MMP-13 contains a TGF-ß inhibiting element (TIE) in its promoter region. TGF-ß is a known pro fibrotic mediator and it has been strongly associated with myocardial remodeling following MI and pressure overload hypertrophy (70). SMADs are important down-stream mediators of the TGF-ß signaling pathway. SMADs are transcription factors that are capable of binding the AP-1 site of the MMP promoter (71). In several studies TGF-ß reduces MMP expression. TGF-ß inhibition of MMP-1 in dermal fibroblasts involves SMAD3 (72). In fibroblasts, ETS1, part of the ETS family capable of binding the PEA-3 binding site of the MMPs promoter region, favors matrix degradation in response to TGF-ß in arthritis and cancer (73). SMADs interact with the AP-1 site of MMP-1, but not with TIMP-1's AP-1 site, and mediate its inactivation by TGF-ß (74). However, Uria et al. reported a stimulation of MMP-13 activity dependent on c-Jun, c-Fos (75). Han et al. have also reported that TNF-α and TGF-β synergistically induce pro MMP-9 in human skin and isolate dermal fibroblasts as well as epidermal keratinocytes

(76). The effect of TGF-ß on MMPs and TIMPs therefore seems to be dependent on concentration and cell type (2).

MMP-13 has been implicated in different cardiovascular disease. Boixel and colleagues identified a trend towards an increase in the expression of interstitial collagenase MMP-13 in atria of infarcted rats (77).
According to Prescott and colleagues, high-fat diet-induced aortic atherosclerosis correlated with an increase in MMP-3, -12, and -13 expression (78). Another study reported an elevated MMP-13 expression in atherosclerotic plaques (79). Furthermore, MMP-13 mRNA expression was increased in a CVB3-induced myocarditis model (80).

Typically, left ventricular remodeling resulting in heart failure is accompanied by changes in structure and composition of the collagen matrix (81) (82) (83). The extent and typology of ECM remodeling varies in between the different etiologies of DCM. In idiopathic DCM there is reduced collagen cross linking, which makes the ECM prone to degradation (81) (84). The loss of ECM contributes to progressive left ventricular dilation and failure. Furthermore, in DCM there is a heterogeneous and continuous ECM turnover (2). EMMPRIN levels are increased in DCM (2). Furthermore, in DCM, upregulation of MMP-2, -3 and -9 has been reported to be combined with a significant decrease in MMP-1 (85). These selective changes in MMP expression profile in DCM are most likely due to transcriptional regulation (2).
Furthermore, left ventricular remodeling is also characterized by formation of reactive oxygen species. Oxidative stress leads to up-regulation of MMPs via post-translational modification of pro MMPs into an active form and the formation of transcriptional complexes which will yield newly formed MMP species (2) (86) (87) (88) (89) (90). Brief incubation of fibroblasts with hydrogen peroxide will significantly increase MMP levels (89). There is a direct relation between the formation of oxidative stress during ischemia/reperfusion and MMP secretion in cardiac surgery (91) (92) (93). Myeloperoxidases are up-regulated in oxidative stress and can cause a transformational change within the MMP-catalytic domain leading to an active enzyme (94) (95).

Moreover, MMP-13 up-regulation is enhanced by Cyr61, as it up-regulates, amongst others, c-Fos, c-Jun and ERK which have binding sites in the MMP-13 promoter regions (96). Cyr61 belongs to the CCN protein family which contains six members CCN1-

CCN6. CCN1 (cyr61-cysteine rich angiogenic inducer 61) regulates a gene program of wound healing by regulating angiogenesis, inflammation and matrix remodeling in dermal fibroblasts (97). Lee et al. have recently shown that activation of FOXO3a causes decreased expression of CCN1 in smooth muscle cells of the vascular wall (96), indicating that FOXO3a can control proteins involved in vascular remodeling.

MATERIALS AND METHODS

MATERIALS

Animals

To prepare neonatal rat cardiac fibroblasts (NRFB) and neonatal rat ventricular myocytes (NRVM), one to three day-old neonatal Wistar Unilever rats were purchased from Forschungseinrichtung für Experimentelle Medizin (FEM) Berlin. FOXO3a -/- and FOXO3a+/+ mouse strains were bred in the Forschungsinstitut für Experimentelle Medizin (FEM) Berlin. Animal studies were reviewed and approved by the Institutional Ethics Committee (SK 176/ 3-1) and were performed according to the General Principles of the Declaration of Helsinki (7th revision of 2013). Animals were grown in constant room temperature of 22°C with humidity of 40-50%, a day-night cycle of 12 hours and they were given free access to water and food.

FOXO3a -/- mice are on an FVB background strain and were generously provided by Prof. DePinho from Dan-Faber-Cancer Center, Boston, MA. *FOXO3a knockout* mice were described previously (98). A schematic representation of the FOXO3a *knockout* gene is indicated in Figure 3.

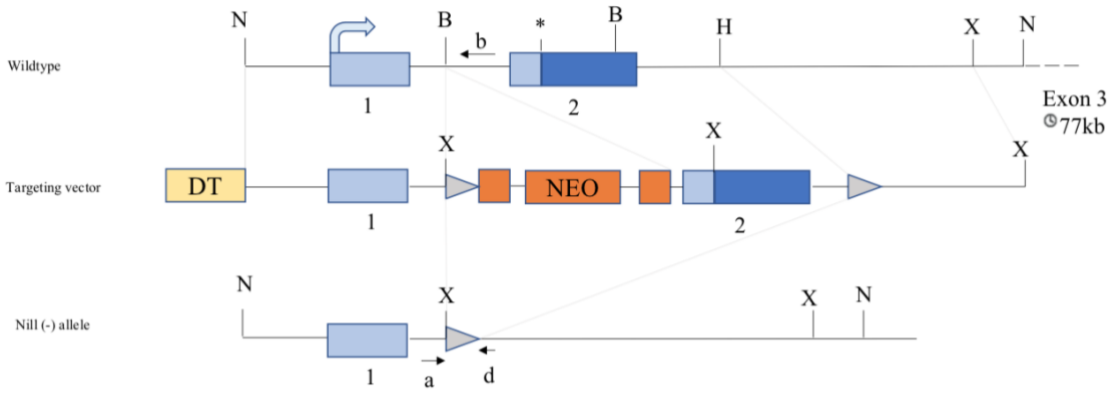

Figure 3: **Targeting strategy for FOXO3a-/- mice.** FOXO3a genomic structure and recombinant alleles. Exon 1 and 2 are shown. Noncoding regions (light blue) and coding region (dark blue, *marks beginning of the region) are indicated. Primers used for PCR are indicated by small arrows. PCR genotyping of wild-type and null alleles was performed using primers a + b + d. DT, diphtheria toxin, Frt sites (empty orange rectangles), loxP sites (grey triangles) (Modified according to Castrillon et al. (98)).

Cell culture, media and supplements

Table 2: Culture media and supplements	
Media/Supplement	**Provider**
Dulbecco's modified Eagles media (DMEM 31885)	Gibco
Fetal calf serum (FCS)	c.c.pro GmbH
Horse serum (HS)	Gibco
Penicillin/Streptomycin (Pen.Strep.)	Sigma Aldrich Chemie GmbH
PBS (no $MgCl_2$, no $CaCl_2$)	Gibco
Gelatine	Sigma Aldrich Chemie GmbH
HBSS (no $MgCl_2$, no $CaCl_2$)	Gibco
0,25 %Trypsin/EDTA Solution	Sigma Aldrich Chemie GmbH
Trypsin 1:250 (powder)	Gibco
Collagenase (type 2)	Worthington
Liberase TH Research Grade	Roche Applied Science
Trypan blue solution	Sigma Aldrich Chemie GmbH
5-Fluoro-2′-deoxyuridine thymidylate synthase inhibitor (FUdR)	Sigma Aldrich Chemie GmbH

Adenoviral vectors and CVB3

AdV5-CMV-GFP, AdV5-CMV-TM-FOXO3a and AdV5-CMV-WT-FOXO3a were used as vectors for the transduction of the NRFBs and NRVMs and are described elsewhere (99). The structure of TM-FOXO3a transgene' s cassette is illustrated in Figure 4. The transcription of the WT-FOXO3a as well as the one of the TM-FOXO3a gene are under the control of a CMV-Promoter. Transgene proteins are both tagged with the hemagglutinin epitope (HA) and all vectors also express the green fluorescence protein marker (GFP), transcriptionally under the control of a CMV-promoter as well.
WT-FOXO3a contains the native Akt inhibitory consensus phosphorylation sites (Thr32, Ser253 and Ser315). The Akt inhibitory phosphorylation sites were substituted by alanine in the TM-FOOX3a protein, therefore rendering TM-FOXO3a constitutively active.

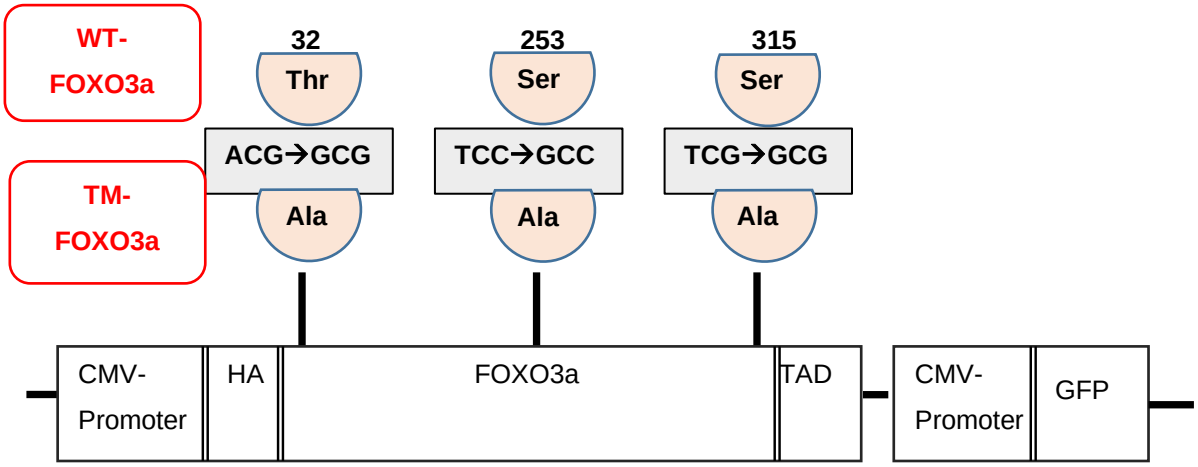

Figure 4: Structure of the transgene regions of the FOXO3a adenoviral vectors. Structure of adenoviral vector transgene regions expressing WT-FOXO3a and TM-FOXO3a. The nucleotide substitutions made to create the non phosphorylatable mutant is indicated. Transgene proteins are tagged with the hemagglutinin epitope (HA), and all vectors also express the green fluorescence protein marker (GFP). TAD, transactivation domain (Modified according to Skurk et al 2004 (99)).

The genetically characterized cardiovirulent Nancy strain of CVB3 was used for viral myocarditis (100). Methods detailing CVB3 propagation in HeLa cell cultures, titration by standard plaque formation assays and storage at – 80°C have been published previously (101).

Kits

Table 3: Kits	
Kit	**Provider**
High capacity cDNA reverse transcription Kit	Applied Biosystems
AmpliTaq Gold	Thermo Fischer
BCA Protein Assay kit	Pierce
SuperSignal™ West Dura Extended Duration Substrate Kit	Thermo Fischer
FastStart Universal Probe Master (ROX)	Roche
Rneasy Mini Kit	Qiagen
Collagenase assay EnzChek Kit+ DQ Collagen type 1 from bovine skin,fluorescein conjugate (#D12060)	Thermo Fischer

Rnase-Free Dnase Set	Qiagen
Dual-Luciferase Reporter Assay System (#E1910)	Promega
Chromatin Immunoprecipitation (ChIP) Assay Kit (17-295)	EMD Millipore

Antibodies

Primary antibodies

Table 4: Primary antibodies		
Target	**Host**	**Provider**
FOXO3a (75D8)	rabbit	Cell Signaling Technology
MMP-13 (H-230)	rabbit	Santa Cruz Biotechnology
MMP-1	rabbit	abcam
TIMP-4	rabbit	abcam
α-tubulin	rabbit	Calbiochem
GAPDH	rabbit	Cell Signaling Technology

Secondary antibodies

Table 5: Secondary antibodies		
Target	**Host**	**Provider**
Rabbit IgG, HRP-linked antibody	goat	Cell Signaling Technology

Inhibitors

Table 6: Inhibitors	
Name	**Provider**
LY294002	Cell Signaling Technology

TaqMan gene expression assays

Table 7: TaqMan™ gene expression assays		
Gene	**Ref. Number**	**Provider**
MMP-13	Rn01448197_m1	Applied Biosystems
MMP-3	Rn00591740_m1	Applied Biosystems
MMP-9	Rn00579162_m1	Applied Biosystems
TIMP-1	Rn00587558_m1	Applied Biosystems

TIMP-2	Rn00573232_m1	Applied Biosystems
HPRT1	Rn01527840_m1	Applied Biosystems
GAPDH	Rn99999916_s1	Applied Biosystems
MMP-13	Mm00439491_m1	Applied Biosystems
GAPDH	Mm99999915_g1	Applied Biosystems

PCR Primers

Table 8: PCR primers		
Primer name	**Sequence**	**Provider**
ratMMP13 #1F	gAACAgAACTTTTCCCTCCTTACA	TIB MolBiol Berlin
ratMMP13 #1R	TTCCTAgTgAgTCgAAggTAAACA	TIB MolBiol Berlin
Primer A Seq.Nr. 1494436	ATTCCTTTggAAATCAACAAAACT	TIB MolBiol Berlin
Primer B Seq.Nr. 1494437	TgCTTTgATACTATTCCACAAACCC	TIB MolBiol Berlin
Primer D Seq.Nr. 1494438	AgAATTATgTTCCCACTTgCTTCCT	TIB MolBiol Berlin

Luciferase Reporter Constructs

Table 9: LightSwitch GoClone Promoter Reporter Construct	
Promoter Construct Name	**Provider**
MMP-13 Promoter Reporter Construct	BioCAT
GAPDH Promoter Reporter Construct	BioCAT

Buffers, solutions and media

Table 10: Buffers, solutions and media	
Name	**Components**
Cell lysisbuffer	10x Cell lysis buffer
	10x PhosphoStop
	7x cOmplete, Mini Protease Inhibitor Cocktail
DNA Digestion buffer	10mM Tris-HCl pH 8
	10mM EDTA pH 8
	50mM NaOH
	0,5% SDS

10x SDS Running buffer	30g Tris base
	144g Glycine
	0,1%SDS for 1x running buffer
1x Transfer buffer	200ml Methanol
	100 ml 10x running buffer
	5ml 20% SDS
1x Blocking solution, antibody dilution solution (5%)	5 mg milk powder
	100ml 1x TBST
10x TBS-Tween solution	200mM Tris base
	1,5M NaCl
	1% Tween 20
6x Protein loading buffer	375mM Tris HCl pH 6,8
	6% SDS
	48% Glycerol
	9% Mercaptoethanol
	0,03% blue Bromophenol
1x Mild stripping buffer	15g Glycine
	1g SDS
	10 ml Tween 20
Trypsin, working solution (sterile filtered) (stock solution: 600µg/ml)	15 mg Trypsin
	25 ml HBSS
Collagenase (type 2), working solution (sterile filtered) (stock solution: 1mg/ml)	50 mg Collagenase
	50 ml HBSS
NRFB culture medium	DMEM
	20% FCS
	1% Pen.Strep.
NRVM culture medium	DMEM
	10% FCS
	10% HS
	1% Pen.Strep.
Serum starvation	DMEM
	1% FCS
	1% Pen.Strep.

2mM FUdR stock solution (2µM for culture medium) (sterile filtered)	5 ml H2O
	2,46 mg FUDR
2% Gelatine solution (autoclaved)	2 g gelatine
	100 ml H2O
10 mM LY294002 stock solution	1,5 mg LY294002
	488 µl DMSO
1% Agarose gel	1,5 g agarose
	150 ml dH_2O
	3 ml 50x TAE
50x TAE buffer	242 g Tris-Base
	57,1 ml acetic acid
	100 ml 0,5M EDTA pH 8,0

Technical equipment, auxiliary material and software

Table 11: Technical equipment and auxiliary materials	
Name	**Provider**
Fridge	Liebherr
Centrifuge 5415R	Eppendorf
Shaker DRS-12	neoLab®
Roller RM5	CAT
Fine scale BP11OS	Sartorius
Thermomixer comfort	Eppendorf
All-In-One Fluorescence Microscope BZ-9000	Keyence
Microplate reader Infinite 200 PRO	Tecan
Microscope DFC480	Leica
Cell counting chamber	Neubauer
Pipettes	Eppendorf
Pipettboy accu	IBS Integra Biosciences
Serological pipettes	Falcon
Micropipette filter tips	Biosphere
Eppendorf tubes	Starstedt
Electrophoresis chamber	Bio-Rad

WB gel holder	Bio-Rad
Schott glass bottles	Schott
Petri dishes	Falcon
Blotting membranes for WB	Thermo Fischer
PVDF membrane	Thermo Fischer
Vortexer	neoLab®
Spectrophotometer	NanoVue Plus IQ/OQ
Magnetic stirrer	IKA
Cell strainer (40µm)	PB Falcon
T75 cell culture flasks	Falcon
96 well-plates black with clear flat bottom	Falcon
96 well-plate white flat bottom	Nunclon Surface
Chemoiluminiscence Imaging System	INTAS
Feather Surgical Blade (stainless steel) no.15 and no. 21	Feather
Surgical instruments	Fine Science Tools
Vasofix Vein Cannula 22 G	B.Braun Melsungen AG
7-0 Ethilon Mono	Ethicon
Sonicator Bioruptor® Standard	diagenode
1,5 ml Bioruptor® Plus TPX microtubes	diagenode
Transilluminator	Biometra
Agarose gel chamber	Bio-Rad

Table 12: Software		
Name	**Application**	**Provider**
Keyence Bio-Viewer	Detection of fluorescent cells	Keyence
icontrol	Data analysis of microplate reader measurements	Tecan
ChemoCam	Detection of chemiluminescence images of immunoblots	Intas
GraphPad Prism 7.0	Statistical analysis	GraphPad
BDA Digital	Image acquisition of agarose gel	Biometra
ImageJ	Data analysis of immunoblots	NIH

Reagents, chemicals and gels

Table 13: Reagents, chemicals, gels	
Name	**Provider**
pre-cast 4-20% SDS gels	BIO-RAD Laboratories
70% Ethanol	Sigma Aldrich Chemie GmbH
beta-Mercaptoethanol	Roth
RNase free water	Ambion
PageRuler Prestained Protein Ladder	Thermo Fischer
Sodium dodecyl sulphate(SDS)	Sigma Aldrich Chemie GmbH
Isofluran 2%	Abbot
Metamizol 500mg/20Ggt	Hexal
HCL	Roth
Tween20	Fischer Scientific
Glycine	Sigma Aldrich Chemie GmbH
Tris/HCl	Roth
NaCl	Roth

Milk powder	Roth
10x Cell lysis buffer	Cell Signaling Technology
cOmplete, Mini Protease Inhibitor Cocktail	Roche
PhosSTOP	Roche
Gelatine	Sigma Aldrich Chemie GmbH
PageRuler Prestained Protein Ladder	Thermo Fischer
FuGENE® HD Transfection Reagent	Promega
protein G-Agarose	Santa Cruz Biotechnology
Roti® Phenol/Chloroform/Isoamyl alcohol	Roth
Chloroform	Merck
Isopropanol	Roth
Ethidium Bromide	Roth
Agarose	SERVA
100mM dNTP for PCR	Invitrogen
Proteinase K	Mechery-Nagel
Acetic acid	Merck
EDTA	Flyka analytical
Tris-Base	Sigma Aldrich Chemie GmbH
Trypan blue	Biochrom
DNA ladder	NEB
DNA loading dye with SDS	NEB
Formaldehyde	Sigma Aldrich Chemie GmbH

METHODS

Animals

Primary neonatal heart cell cultures were prepared from cardiac tissue of one to three-day-old Wistar Unilever rat pups. Rats were euthanized by decapitation after shortly being dipped in 70% ethanol. The removed hearts were placed into a Petri dish containing ice-cold Hanks Buffered Salt Solution (HBSS).

Cell culture

All cell culture work was performed in a laminar flow hood under appropriate aseptic conditions.

Primary neonatal rat cardiac myocytes and fibroblasts

The excised rat hearts were transferred to another Petri dish and minced into pieces using two sterile scalpels. Two digestion steps were performed to obtain cardiac cells. The first digestion step was performed overnight at 4°C under gentle agitation by incubation of the cardiac tissue with trypsin solution. The second digestion was performed stepwise using an HBSS solution containing 1mg/ml of Collagenase (type 2) (Worthington) until the tissue was completely dissolved. Each step was performed at 37°C for 5 min under continuous and moderate mixing with a sterile magnetic stirrer in a 50 ml beaker containing 5 ml of the Collagenase (type 2) solution. After each step the suspension was collected and introduced into an ice-cold falcon tube. The content of the falcon tube was then filtered through autoclaved gauzes into a new falcon tube. Cells were pelleted after centrifugation at 1200rpm for 5min at 20°C. NRFB culture medium was used to resuspend the cell pellet and incubate it for 90 min at 37°C with 5% CO2 until the non-myocyte fraction sedimented. The attached cells, mainly cardiac fibroblasts, were then cultured in proper medium, grown to confluence and passaged at 1:3 yielding almost pure cardiac fibroblasts after the first passage. Culture medium was changed every other day. All experiments with neonatal rat cardiac fibroblasts were carried out after passages 1 to 3. The non-sedimented viable cells enriched in cardiac

myocytes were removed, centrifuged at 1200rpm for 5 min at 20°C and seeded in gelatin pre-coated plates for experiments in proper culture medium. To inhibit proliferation of contaminating non-myocytes 2 µM FUdR was present in culture medium throughout the whole NRVM culture period. Growth medium was exchanged daily and biochemical analyses were performed at culture day three when cardiomyocytes had formed a synchronously contracting monolayer. The spontaneous contraction rate and photographic documentation of the growing cardiomyocytes were monitored before each medium exchange using an inverse phase contrast microscope. This protocol provided constantly cell populations containing 90 to 95% cardiac myocytes. All cell culture mediums, supplements and solutions are listed in Table 2 and 10.

Primary murine cardiac fibroblasts

For these experiments, FOXO3a *knockout* and *wildtype* FVB mice were used at the age of six to eight weeks. The hearts of the animals were removed, minced with scissors and placed in cold HBSS (Hank's balanced salt solution). The tissue was disrupted in 5 ml of HBSS supplemented with 100 µg / ml Liberase TH Research Grade (collagenase I and II, thermolysin) at 37 ° with stirring. The supernatant was removed and collected approximately every ten minutes and fresh tissue was added to the residual tissue until the tissue was completely dissolved. The cell suspension was then filtered by means of a cell filter with a pore size of 40 µm, centrifuged at 600 g for five minutes and cultured in DMEM with 10% FBS and 1% P.S for 120 minutes in cell culture dishes at 37 ° C. After the fibroblasts sedimented, the supernatant was pipetted off and the cardiomyocyte cell culture was established using the sediment. The culture medium consisted of DMEM spiked with 10% FBS and 1% P.S. The fibroblasts were grown to confluency in cell culture vessels and passaged in a 1:3 distribution. The morphological characterization revealed a fibroblast content of >95% after the first passage. All experiments with cardiac fibroblasts were performed after the first or second passage. All necessary materials are listed in Table 2, 10 and 11.

Trypan Blue exclusion test

Cell viability and cell number of isolated primary NRFBs and NRVMs were assessed using the trypan blue exclusion test. Viable cells exclude trypan blue due to their intact cell membranes and appear uncolored, whereas dead cells are colored blue after the dye diffused into them. 50µl cell suspension was incubated with 50µl trypan blue 0,5% solution for one minute at RT. After that, viable and dead cells were counted in a Neubauer Counting Chamber and the viability, the number of living cells per ml, and the total amount of viable cells were calculated. Cell suspensions with a viability greater than 85% were used for further experiments. All necessary materials are listed in Table 2, 10 and 11. Table 14 indicated seeding densities per cell type.

Table 14: Seeding densities/well for NRFB and NRVM			
NRFB		**NRVM**	
6 well-plate	800.000 cells/well	6 well-plate	1.200.000 cells/well
12 well-plate	250.000 cells/well	12 well-plate	600.000 cells/well
96 well-plate	20.000 cells/well		

Transduction of primary NRFB and NRVM

Adenoviral vector solutions with AdV5-CMV-GFP, AdV5-CMV-TM-FOXO3a or AdV5-CMV-WT-FOXO3a were prepared by diluting the vector in a culture medium without supplements. Prior to transduction, the medium was removed and cells were washed once with PBS. Fresh medium was then added to the seeded cells and 100µl of adenoviral vector solution was dropwise pipetted to each well in cells seeded in 6 and 12 well-plates. 20µl of diluted adenoviral vector was used for the transduction of cells in 96 well-plates. Cells were incubated with a different multiplicity of infection (MOI) according to experimental layouts. NRFB were incubated with 5 and 10 MOI. NRVM were incubated with 20 and 40 MOI. After incubation, the medium was removed and cells were washed once with PBS. After each transduction, the expression of green fluorescent protein was checked under a fluorescence microscope (Keyence BZ-9000)

with a 540nm filter applied. Transduction efficacy was > 90% for all cell cultures used in the present study. Thereafter, biochemical analyses were performed. The transduction efficiency was calculated in percentage as the number of cells expressing GFP divided by the total number of cells present. All necessary materials are listed in Table 2, 10, 11 and 12.

In vivo cardiac injury models to investigate cardiac matrix remodeling

CVB3-induced myocarditis

Six- to eight-week old male FVB *wildtype* and *knockout* mice were infected with $5x10^4$ plaque-forming units (pfu) of CVB3 intraperitoneally. Three days after infection mice were sacrificed and hearts were harvested for biochemical analysis. Mice were analyzed on day seven, hearts were removed and snap frozen.

Murine models of myocardial infarction

To investigate remodeling after ischemic damage to cardiac tissue, an *in vivo* model of myocardial infarction was applied in C57BL/6J FOXO3a *wildtype* mice (Jackson Laboratories). Induction of myocardial infarction was achieved by surgical ligation of LAD (102). After induction of anesthesia with 2% isoflurane, mice were intubated with a 22G-cannula and ventilated with isoflurane 2% to maintain the anesthesia. The thoracotomy was performed in the 2^{nd} left intercostal space. The ligation of the LAD took place at a distance of 2-3mm from the main stem via 7-0 Etibond thread. Finally, an over-inflation of the lungs with the help of the ventilator was performed to eliminate residual air from the thoracic space and finally the chest was closed by means of suture. The operations of the Sham animals were carried out according to the same protocol including thoracotomy, without ligature of the LAD. Postoperatively, p.o. analgesia was administered using 500mg/ml of Metamizol as 1-2 drops into the oral cavity (200 mg/kg bw) after surgery and subsequently as drinking water (200 mg / kg bw) every six hours until the time of sacrifice. This was performed on day three postoperatively by means of manual cervical dislocation. The hearts were removed, tissue taken from both the infarct scar and infarcted myocardium and stored at -80°C until molecular biology studies were performed.

Murine models of Coxsackievirus B3 (CVB3)-induced myocarditis

The CVB3 model was implemented in six to eight- week old FOXO3a-KO mice and FVB wild-type mice as described in Jenke et al. (103). Induction of CVB3 myocarditis was initiated and maintained by inhalation of isoflurane 2% and intraperitoneal injection of $5x10^5$ plaque forming units of transfection-derived and purified coxsackievirus B3 (Nancy strain, ATCC) into 200µl PBS Number: VR-30, provided by Prof. K. Klingel, (University of Tübingen) (104). The control group received 200 µl of PBS intraperitoneally. The killing took place on day seven after intraperitoneal injection/infection by means of manual cervical dislocation. To detect the infection, a PCR was carried out, with a number of CVB3-positive cDNA copies of 103/ng cDNA from the left ventricle serving as the limit for inclusion in the present work.

Molecular biology

Genotyping

Genotyping was performed to determine the genetic variation amongst *wildtype* and *knockout* mice. Initially DNA was extracted from ear clips and afterwards, PCR was performed to amplify the DNA of each sample. Finally, amplified samples were run in a 1% agarose gel and images were obtained using a transilluminator. All necessary materials for all the steps of genotyping are listed in Table 3, 7, 10, 11, 12 and 13.

DNA extraction from ears of *wildtype* and *knockout* mice

Approximately 0,5 cm of ear clip of each mouse was removed and transferred to a polypropylene tube. DNA Digestion Buffer was heated for ten minutes at 75°C to inactivate the DNase and brought to room temperature. Proteinase K was added at a final concentration of 0,5 mg/ml. 200µl of the DNA Digestion Buffer and Proteinase K mixture was added to each sample and incubated at 55°C for 30 min. 250µl of phenol/chloroform/isoamyl alcohol was added and vigorously mixed. All samples were then centrifuged at 15000g for five min. at room temperature. The aqueous phase was carefully transferred to a new tube. Subsequently, 250µl of chloroform was added and mixed with hands. Samples were then centrifuged at 15000g for five min. at room

temperature. The aqueous phase was carefully removed and transferred to a new tube. 200µl of isopropanol was added and mixed with hands. Samples were then incubated at -20°C for two hours. After that, samples were centrifuged at 15000g for ten min. at 4°C. The supernatant was carefully removed and 500µl of 70% freshly prepared ethanol was added. To wash the pellet, the tube was flipped once manually. Samples were centrifuged once more at 15000g for ten min. at 4°C and then let air dry for no more than ten min. Next, the pellet was resuspended in 90µl nuclease-free water and samples were incubated at 55°C for 30 min. under gentle agitation. Samples were then stored at -20°C until further analyses were performed.

PCR

DNA extracted from the samples was amplified to achieve allelic discrimination by running a PCR reaction using AmpliTaq Gold (Thermo Fischer). Samples were placed on ice and Buffer Gold, dNTPs, MgCl2, Primer A, B, D, TaqGold and nuclease-free water were added. Table 15 indicates the composition of the genotyping PCR reaction. Samples were then placed in the machine and the RT-PCR was run. Specific sequences complementary to the primers in the RT-PCR reaction are amplified. These primers refer to sequences in the FOXO3a *wildtype* and null allele gene. Initially, the rise in temperature allows the activation of the TaqGold polymerase and the denaturating of the DNA double strand. The annealing phase follows, where primers bind to their complementary sequences in the extracted DNA. The TaqGold polymerase then adds complementary nucleotides to extend the complementary DNA strand. The genotyping PCR program is indicated in Table 16. After the PCR was performed, the samples were stored at -20°C.

Table 15: Genotyping PCR reaction composition	
Master Mix	**Volume/sample (µl)**
10x Buffer Gold	2
25x dNTP Mix 100mM	3,2
MgCl2	2
Primer A	0,26
Primer B	0,13
Primer D	0,26

Taq Gold	0,1
RNase free H2O	9,7

Table 16: Genotyping PCR program		
Cycle	**Target temperature**	**Hold time**
1	94°C	5 min
40	94°C	30 sec
	59°C	1 min
	72°C	1 min
1	72°C	10 min

1% agarose gel for detection of the genotype

DNA is negatively charged and, by applying an electric field, it can be separated by size in the agarose gel matrix. The amplified samples were run in a 1% (1g/100ml) agarose gel. The agarose was boiled in 1xTAE buffer. After the agarose solution became clear, ethidium bromide was added to the gel mixture and carefully poured into a gel chamber until it polymerized. The samples were then mixed with 6x loading buffer and pipetted into the wells along with the DNA ladder. The gel was let run for 1 hour and 30 min at 100V. After the gel had run, images were obtained using a transilluminator (Biometra).

RNA isolation

The RNeasy Mini kit from Qiagen was used. For RNA isolation from primary cell lines, the cells were seeded in 12 well plates. After performing the experiments, culture medium was removed, cells were washed with PBS. For RNA isolation from tissues isolated from the myocardial infarction and myocarditis *in vivo* models, tissue samples were cut into slices less than 0.5 cm thick.

RNA isolation was then performed according to manufacturer's protocol. To eluate the purified RNA, 30µl of RNase-free water was used. RNA concentration was then measured with NanoVue Plus device using an absorption at 260nm. RNA was stored at -80°C. All necessary materials are listed in Table 3, 11, 12 and 13.

cDNA Synthesis

The cDNA synthesis was performed using High-Capacity cDNA Reverse Transcription kit (Applied Biosystems), starting with 1 µg RNA in a 10 µl reaction system. First the extracted RNA was incubated for 10 min at 70°C. The samples were then placed on ice, and Master Mix, RT Buffer, dNTP Mix, RT Random Primers, MultiScribe RT and RNase-free water were added and mixed accordingly (Table 17). Samples were then incubated at 37°C for two hours to perform the cDNA synthesis. cDNA (complimentary DNA) is synthesized from a single stranded RNA template in a reaction catalyzed by the enzyme reverse transcriptase. Random hexamer primers, contained in the kit, contain every possible 6-base single strand of DNA and can therefore hybridize anywhere on the RNA. All necessary materials are listed in Table 3, 8, 11, 12 and 13. After the cDNA synthesis was performed, the samples were stored at-20°C.

Table 17: cDNA Master Mix composition	
Master Mix	**Volume/sample (µl)**
10x RT Buffer	2
25x dNTP Mix 100mM	0,8
10x RT Random Primers	2
Multiscribe RT reverse transcriptase (50U/µl)	1
RNase-free H2O	0,2

Quantitative Real Time PCR (TaqManTM)

In this step, the DNA polymerase amplifies target cDNA using sequence-specific primers, cleaving the TaqMan® probe to generate a fluorescent signal that is measured by the real-time PCR system. FastStart Taq DNA Polymerase is a chemically modified form of thermostable recombinant Taq DNA Polymerase that shows no activity up to +75°C. The enzyme is active only at high temperatures, where primers no longer bind non-specifically. The enzyme is completely activated (by removal of blocking groups) in a single pre-incubation step (+95°C, 10 min) before cycling begins (Table 19). Total RNA from cells was extracted with RNeasy Mini Kit (Qiagen) according to manufacturer's instructions. 1µg of RNA was used as a template to synthesize cDNA,

using the High capacity cDNA Reverse Transcription Kit (Applied Biosystems). Quantitative RT-PCR reactions were set up as recommended by the manufacturer. FastStart Universal Probe Master mix (ROX) (Roche) and TaqMan™ gene expression assays (Applied Biosystems) were used (Table 18). Target amplification using cDNA as the template is the second step in the two-step RT-PCR. HPRT1 and GAPDH (Applied Biosystems) was used as an endogenous control. Ninety-six well microplates were run and analyzed on the Applied Biosystems qPCR machine. Results were expressed as mean-fold changes of gene expression relative to HPRT1 expression using the $2^{-\Delta\Delta CT}$ method. All necessary materials are listed in Table 3, 7, 10, 11, 12 and 13.

Table 18: TaqMan™ qRT-PCR reaction mix composition	
Component	**Volume/reaction**
FastStart Universal Probe Master (ROX)	5 µl
TaqMan™ gene expression probe	0,5 µl
RNase-free H2O	3,5 µl
cDNA	1 µl

Table 19: qRT-PCR program		
Cycle	**Target temperature**	**Hold time**
1	50°C	2 min
1	95°C	10 min
40	95°C	15 sec
	60°C	1 min

Proteomics

Protein isolation and quantification

Protein from cells was extracted using 90µl/well of Cell Lysis Buffer (Cell Signaling Technology) supplemented with proteinase and phosphatase inhibitors to inhibit proteases and to preserve the phosphorylation pattern of cellular proteins (PhosSTOP and cOmplete, Mini Protease Inhibitor Cocktail from Roche). Cells were then scraped and the content was introduced into a 1,5ml Eppendorf tube.

Protein from the infarcted area of *wildtype* and *knockout* mice was extracted by adding 300µl of Cell Lysis Buffer (Cell Signaling Technology) supplemented with proteinase and phosphatase inhibitors to inhibit proteases and to preserve the phosphorylation pattern of cellular proteins (PhosSTOP and cOmplete, Mini Protease Inhibitor Cocktail from Roche) to 5mg of tissue. The samples were introduced into 1,5ml Eppendorf tube and placed on ice. They were maintained under constant agitation for 2h to allow for the lysis of the tissue.

To remove cellular debris, the tubes containing samples either from cells or tissue were centrifuged at 15000g for 15 min. at 4°C. The supernatant was transferred to a fresh tube and protein was then quantified with a bicinchoninic acid (BCA) assay (Thermo Fischer). The BCA Protein Assay uses a detergent-compatible formulation based on bicinchoninic acid (BCA) for the colorimetric detection and quantitation of total protein. The reduction of Cu^{+2} to Cu^{+1} by protein in an alkaline medium (the biuret reaction) is combined with the detection of the cuprous cation (Cu^{+1}). Concentration was measured against the BSA standard with a microplate reader device (Infinite 200 PRO) at an absorbance of 560nm. All necessary materials are listed in Table 3, 10, 11, 12 and 13.

Western Blot

20µg of protein was mixed with 6x SDS sample buffer (loading buffer) and incubated at 95°C for ten minutes. Samples were loaded onto a 4-20 % SDS precast ready-made gel (Bio-Rad Laboratories). Electrophoretic separation of the proteins was performed at 100V using a Bio-Rad WB chamber in 1x running buffer. 10µl of PageRuler Prestained Protein Ladder (Thermo Fischer) was used as the molecular weight standard to estimate protein size.
The PVDF membrane (0,2µm) (Thermo Fischer) was activated in methanol for two-three minutes and the gel blotted at 100V for 90 min. in 1x transfer buffer. Blotted membranes were incubated with blocking solution for 1h at room temperature to block unspecific biding, Afterwards, they were incubated with primary antibodies, diluted in 5% milk solution, specific for the protein of interest over night at 4°C rotating. Blots were washed three times for ten minutes with 1x TBS-T and then incubated with the secondary antibody diluted in 1x TBS-Tween 5% milk powder solution for 1h at room temperature rotating. Three subsequent washing steps with 1x TBS-T for ten minutes and another two with

PBS for ten minutes followed. Specific detection of protein bands via chemiluminescence was achieved by using the Super Signal Dura West kit (Thermo Fisher) and the Chemoilluminescence Imager (Intas). All necessary materials are listed in Table 4, 5, 10, 11, 12 and 13.

Collagenase assay

NRFBs were cultured in 96 well-plates and transduced for 24h with AdV5-CMV-GFP or AdV5-CMV-TM-FOXO3a. Supernatant was collected and stored at -80°C prior to the assay. The EnzChek kit was purchased from Thermo Fischer. DQ collagen Type I is heavily labeled with fluorescein. When the collagenase cleaves DQ collagen Type I, the fluorescein is quenched. In this assay, the increase in fluorescence is proportional to proteolytic activity. The assay was performed using black clear flat bottom 96 well-plates from Falcon. DQ collagen fluorescence was measured in a micro plate reader (Infinite 200 PRO) with absorption maxima at 495 nm and fluorescence emission maxima at 515 nm according to manufacturer's protocol. All necessary materials are listed in Table 2, 3, 10, 11, 12 and 13.

Chromatin Immunoprecipitation Assay (CHIP)

Chromatin Immunoprecipitation was performed using the Chromatin Immunoprecipitation (ChIP) Assay Kit from Upstate (Millipore). NRVM were cultivated in the presence or absence of serum or transduced with an adenoviral vector expressing either AdV5-CMV-GFP (control) or AdV5-CMV-TM-FOXO3a. FOXO3a/DNA complexes were cross-linked using formaldehyde. After cross-linking, the samples were sonicated. The sonication was performed using Bioruptor® Standard sonicator. 2 ON/OFF cycles of 30 sec were used to generate DNA fragments between 200 and 1000 bp. For DNA shearing, 1,5 ml TPX tubes (diagenode) were used. Subsequently, immunoprecipitation was performed using rabbit polyclonal IgG anti-FOXO3a antibody (1:100, 75D8, Cell Signaling Technology), and protein G-Agarose (Santa Cruz Biotechnology). The same material without using antibody served as control. After reversing protein-DNA-cross-links for four hours at 65°C, DNA was eluated and samples were analysed by PCR for the FOXO3a-bound MMP-13 promoter region containing identified FOXO3a binding sites (Primer F:gAA Cag AAC TTT TCC CTC CTT ACA, Primer R: TTC CTA gTg AgT

CgA Agg TAA ACA). Samples were then run in a 1% agarose gel for approximately 1h and 30min with 100V. Input represents cross-linked DNA amplified without immunoprecipitation with respective antibodies and serves as loading control. Figure 5 illustrates the ChIP Assay procedure. All necessary materials are listed in Table 2, 3, 10, 11, 12 and 13.

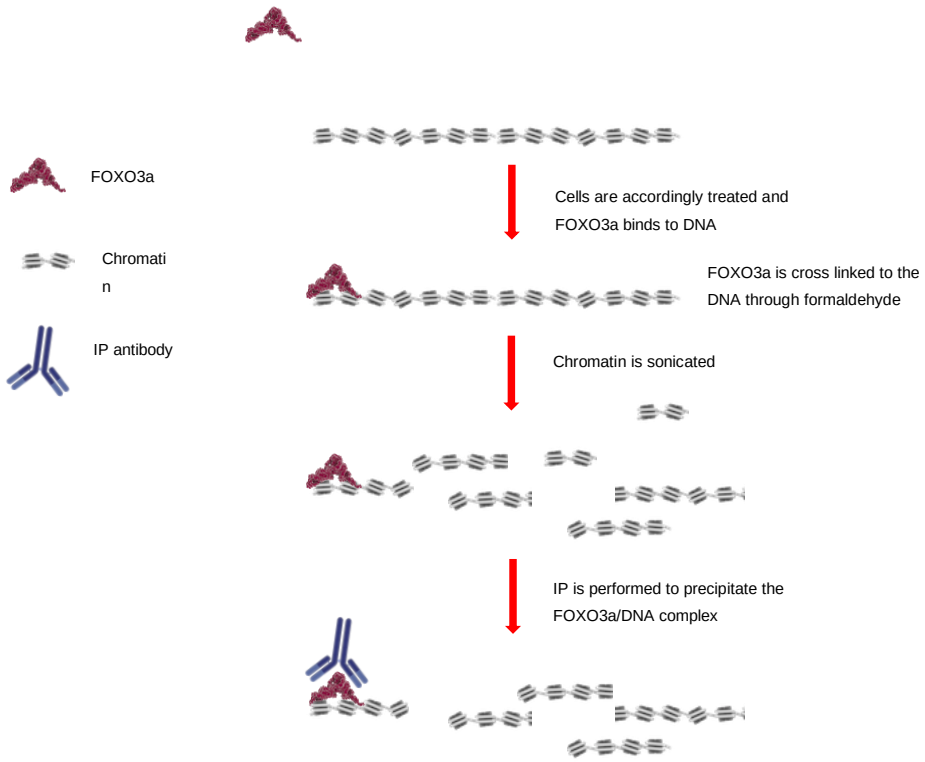

Figure 5: Illustration of ChIP Assay procedure. FOXO3a/DNA complex was cross-linked using formaldehyde. Cell lysates were obtained and sonication was performed. 200-1000 bp DNA fragments were obtained. IP was then performed to extract the cross-linked FOXO3a bound to the DNA.

Luciferase Promoter assay

NRVM were cultured in 6-well chambers and transduced with replication-deficient adenoviral vectors as indicated overnight. LightSwitch GoClone Promoter Reporter Constructs expressing Renilla Luciferase under the control of the rat MMP-13 promoter,or of the control promoter for housekeeping gene GAPDH, were purchased

from BioCat. Transient transfection of the respective promoter-luciferase reporter constructs was carried out using FuGENE HD Transfection Reagent (Roche). Cell extracts were prepared 4h post-transfection. Luciferase reporter activity was assessed on a luminometer as suggested by the manufacturer. MMP-13 promoter controlled renilla activity was normalized to the control promoter activity. All necessary materials are listed in Table 2, 3, 9, 10, 11, 12 and 13.

Statistical analysis

Graphs and statistical analysis were made with GraphPad Prism version 7.0 software. The student's *t*-test unpaired comparison was used to determine any significant differences between each group. *P*-values < 0,05 were considered to be significant.

RESULTS

NRFB and NRVM transduced with AdV5-CMV-GFP, AdV5-CMV-WT-FOXO3a or AdV5-CMV-TM-FOXO3a express FOXO3a protein.

FOXO3a undergoes strict functional control at its phosphorylation sites by its up-stream regulators under different cellular conditions. To be able to study the effects of FOXO3a on matricellular remodeling, gains in function adenoviral vectors were employed, encoding either WT-FOXO3a or TM-FOXO3a under the control of a CMV promoter. Both vectors express GFP. TM-FOXO3a has each of the three Akt phosphorylation sites replaced by alanine. Therefore, TM-FOXO3a is constitutively active. Replication defective adenoviral vectors encoding for GFP under a CMV promoter were used as control vectors.

Initially, transduction efficiency of adenoviral vectors in cardiac fibroblasts and cardiomyocytes in the presence of growth factors was evaluated using fluorescent microscopy at a wavelength of 540nm. Transduction was determined 12 and 24 hours post-infection by the expression of green fluorescent protein (GFP). Figure 6A represents images of sub-confluent NRFB and NRVM transduced with AdV5-CMV-GFP. As indicated in the graph in Figure 6A, GFP transduction efficiencies in neonatal cardiac fibroblasts were 89% for an MOI of five and in neonatal cardiomyocytes greater than 92% for an MOI of 20. When transduced for 24 hours, both cell types showed no apparent sign of apoptosis. Transduction with AdV5-CMV-WT-FOXO3a and AdV5-CMV-TM-FOXO3a showed no significant difference in both cell types in terms of GFP transduction efficiency when compared to transduction with AdV5-CMV-GFP (data not shown).

In addition, whole cell lysates from the same cells were used to perform western blots to verify TM-FOXO3a and WT-FOXO3a protein expression. Neonatal rat cardiomyocytes (NRVM) were transduced with adenoviral vectors with a multiplicity of infection (MOI) of 20 and 40 overnight. FOXO3a protein expression was assessed by western blotting and alpha-tubulin was used as a loading control. Figure 6C represents WT-FOXO3a and TM-FOXO3a expression in NRVMs under normal growth conditions. In the presence of growth factors, a dose-dependent up-regulation of FOXO3a protein expression was confirmed in NRVMs transduced with AdV5-CMV-WT-FOXO3a and AdV5-CMV-TM-

FOXO3a. Phosphorylated, e.g. functionally inactive FOXO3a protein expression (FOXO3aThr32) was identified in cells transduced with AdV5-CMV-WT-FOXO3a, confirming the presence of susceptible phosphorylation sites to growth-factor/PI3k/Akt signaling in the WT-FOXO3a protein.

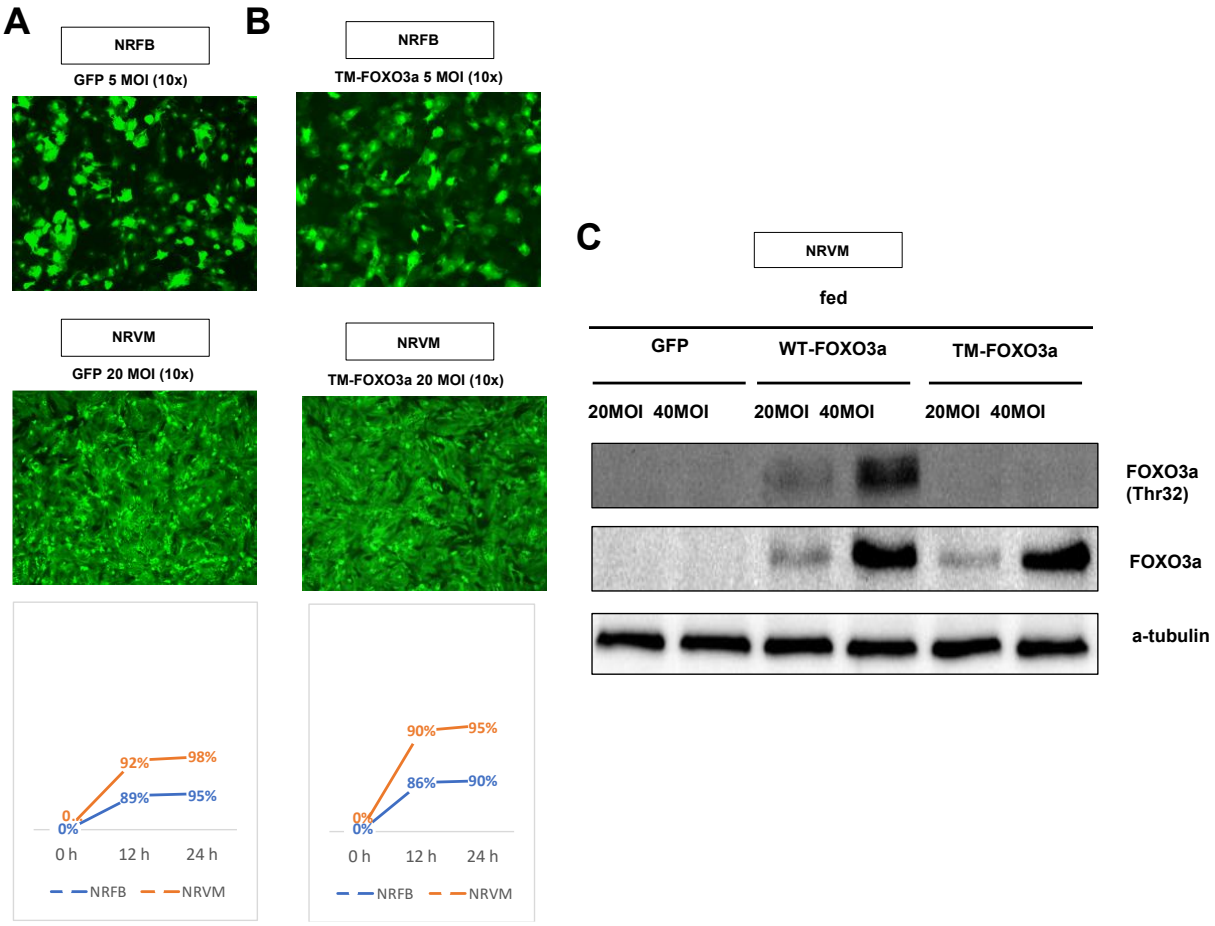

Figure 6: Adenoviral vector transduction efficiency and exogenous FOXO3a expression. Sub-confluent NRFBs and NRVMs were transduced overnight with A) AdV5-CMV-GFP and B) AdV5-CMV-TM-FOXO3a and images shown were taken after 24 h. The graphs indicate temporal distribution of the transduction efficiency of A) GFP and B) TM-FOXO3a. C)FOXO3a total protein and inactive FOXO3a (Thr32) expression of the same cells was detected through western blotting. Baseline FOXO3a protein expression was increased in NRVMs after transduction. WT-FOXO3a was phosphorylatable by Akt under normal growth conditions, in contrast to TM-FOXO3a. A representative blot is shown. Three experiments in triplicates were performed.

However, although overexpression of the TM-FOXO3a transgene was confirmed by immunoblots for FOXO3a in a dose-dependent manner (as shown in Figure 6C) no signal for Thr32 phosphorylation was detected following serum stimulation, indicating expression of the functionally active (i.e. alanine mutated, non-phosphorylable) form of FOXO3a.

Effects of FOXO3a on myocardial MMPs and their inhibitors in NRVM

To initially identify whether FOXO3a influences expression of common cardiac ECM regulators, mRNA and protein expression was performed as an initial screening, following endogenous FOXO3a activation or FOXO3a gain of function transduction. Cardiac cells were cultured under conditions that favored FOXO3a activation or inactivation, i.e. in the absence or presence of growth factors or transduced with either AdV5-CMV-GFP, AdV5-CMV-WT-FOXO3a or AdV5-CMV-TM-FOXO3a. As indicated in Figure 7A-B, there was no significant difference in the mRNA expression of MMP-3 or MMP-9 in serum starved cardiomyocytes (i.e. FBS 1%) or in those cultured in the presence of growth factors (i.e. FBS 10% + HS 10%). Moreover, expression levels of MMP-3 and MMP-9 following transduction with AdV5-CMV-GFP or AdV5-CMV-WT-FOXO3a in serum starved cells were not significantly different. Furthermore, following transduction with AdV5-CMV-GFP, AdV5-CMV-TM-FOXO3a or AdV5-CMV-WT-FOXO3a, MMP-1 protein expression was assessed in NRVMs. A constitutive FOXO3a did not up-regulate MMP-1 protein expression (Figure 7C). The effect of exogenous and endogenous FOXO3a on TIMPs was assessed in NRVMs. TIMP-1 and TIMP-2 mRNA assessment showed no significant difference in NRVMs, grown under normal conditions or serum starvation, i.e., FOXO3a activation. Furthermore, transduction with AdV5-CMV-WT-FOXO3a did not show a significant dose-responsive difference in serum starved cells (Figure 8A and Figure 8B). NRVMs were transduced with replication deficient adenoviral vectors encoding either for WT-FOXO3a or for TM-FOXO3a, and protein expression of TIMP-4 was determined. Immunoblots showed a TIMP-4 baseline protein expression in cardiomyocytes that was not differentially expressed following exogenous FOXO3a overexpression (Figure 8C). Taken together, endogenous and exogenous FOXO3a was unable to modulate the expression of common regulators of cell-matrix interaction.

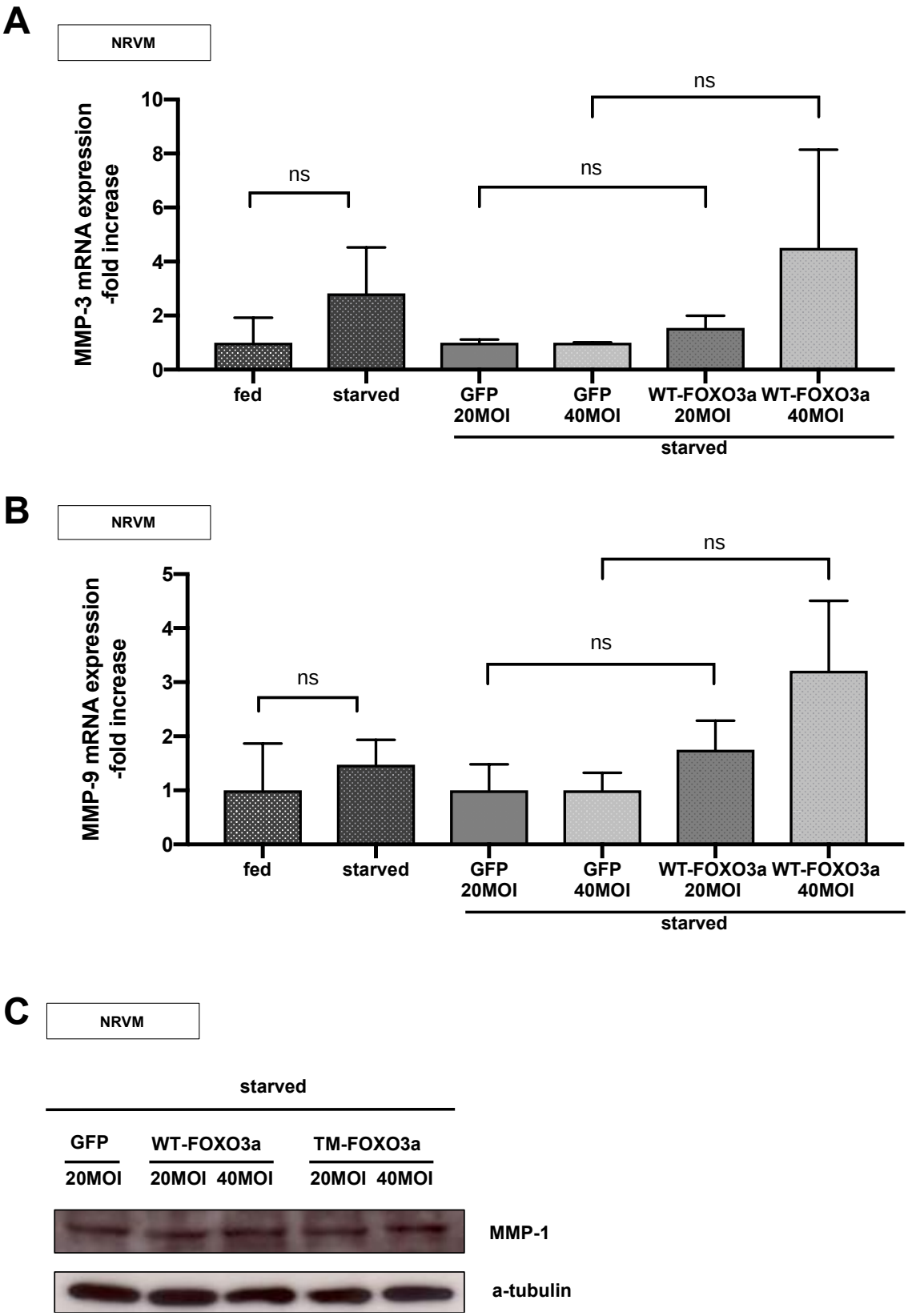

Figure 7: Exogenous and endogenous FOXO3a influence on cardiac ECM regulators. NRVMs were transduced or serum starved and A) MMP-3 and B) MMP-9 mRNA expression was assessed. No significant difference was observed in NRVMs. C) MMP-1 protein expression in NRVMs transduced with adenoviral vectors encoding for GFP, WT-FOXO3a or TM-FOXO3a. Baseline MMP-1 content was not affected by WT-FOXO3a or TM-FOXO3a. The bar graph illustrates data as Mean±SE for three independent experiments in triplicates. A representative immunoblot is shown.

Additionally, MMP-13, an MMP playing an important role in cardiac remodeling, was included in the screening. Interestingly, in comparison to other ECM regulators, MMP-13 expression was significantly up-regulated by constitutively active FOXO3a overexpression in NRFB (Figure 9A). This effect of FOXO3a on MMP-13 was also assessed in NRVM. A significant dose-dependent up-regulation of MMP13 mRNA expression following TM-FOXO3a transduction was confirmed (Figure 9B). In accordance with these data, a significant up-regulation of MMP-13 protein expression was observed in NRVMs following TM-FOXO3a gene transfer, while under conditions of serum stimulation, WT-FOXO3a did not exhibit any effect (Fig. 9C).
Taken together, FOXO3a positively affects MMP-13 expression in cardiomyocytes and fibroblasts of neonatal rats.

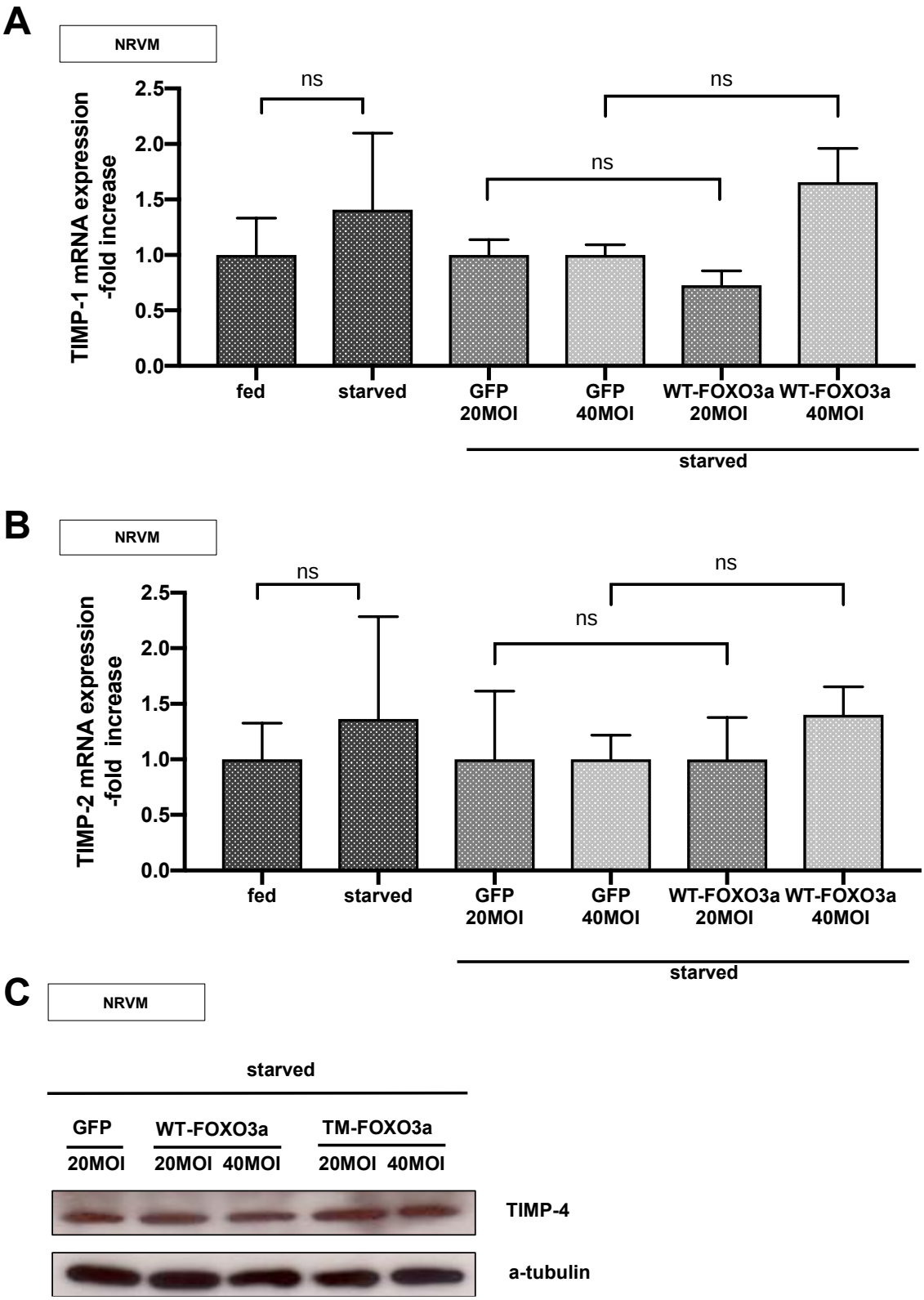

Figure 8: Exogenous and endogenous FOXO3a influences cardiac ECM regulator expression. NRVM were transduced or serum starved and A) TIMP-1 and B) TIMP-2 mRNA expression was assessed. No significant difference was observed in NRVMs. C) TIMP-4 protein expression in NRVMs transduced with adenoviral vectors encoding for GFP, WT-FOXO3a or TM-FOXO3a. Baseline TIMP-4 content was not affected, neither by WT-FOXO3a nor TM-FOXO3a. The bar graph illustrating data as Mean±SE for three independent experiments in triplicates. A representative immunoblot is shown.

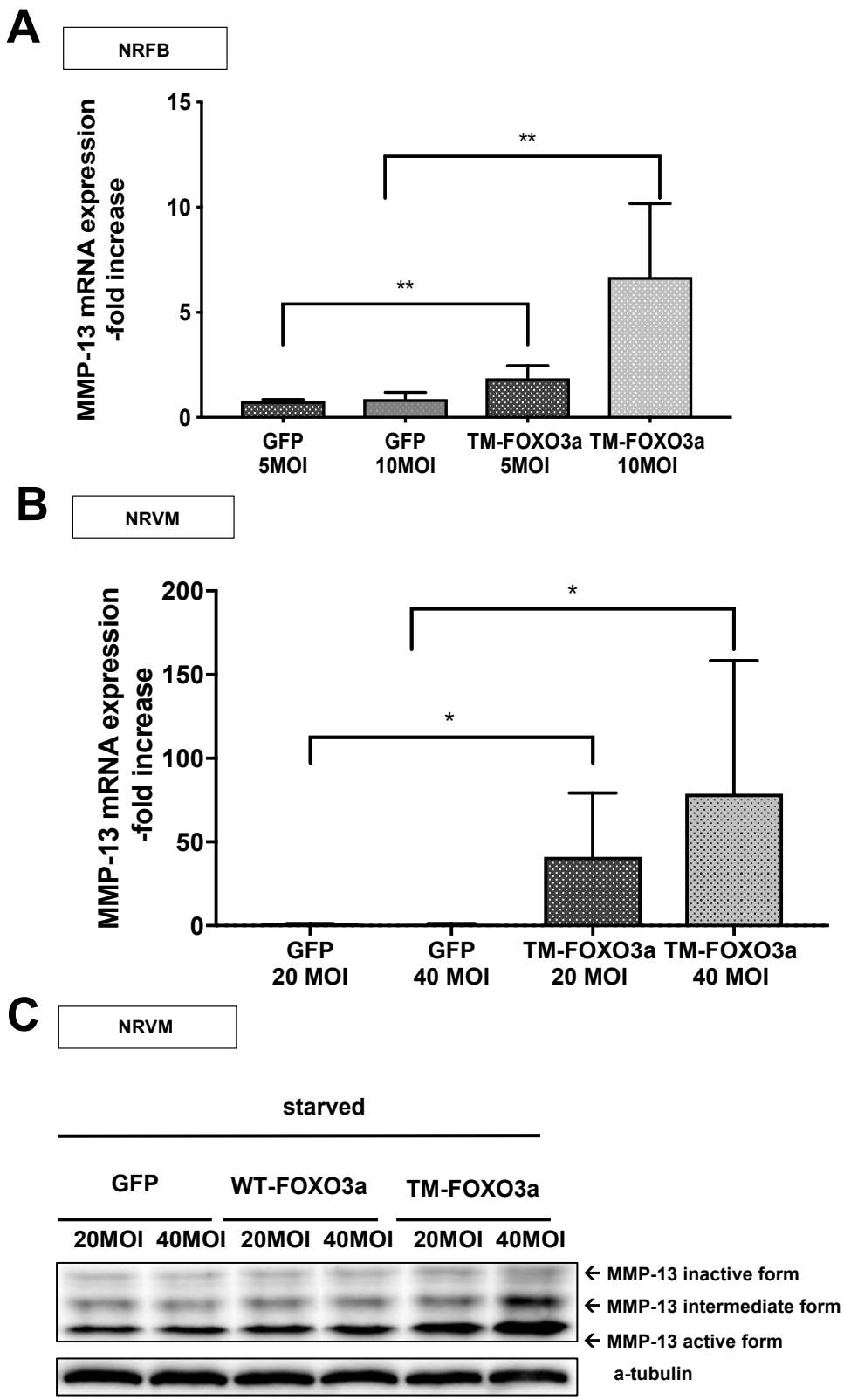

Figure 9: Exogenous FOXO3a up-regulates on cardiac MMP-13 expression. A) NRFBs and B) NRVMs were transduced with AdV5-CMV-GFP or AdV5-CMV-TM-FOXO3a and mRNA expression of MMP-13 was assessed. TM-FOXO3a dose-dependently up-regulates MMP-13 mRNA expression. C) MMP-13 protein expression in NRVMs transduced with adenoviral vectors encoding for GFP, WT-FOXO3a or TM-FOXO3a. MMP-13 content was up-regulated by TM-FOXO3a in a dose-dependent manner. The bar graph illustrates MMP-13 mRNA expression as Mean±SE for three independent experiments in triplicates (*$p<0.05$, **$p<0.01$). A representative immunoblot is shown, three independent experiments in triplicates were performed.

Endogenous FOXO3a-MMP-13 regulation through Akt in cardiomyocytes.

To further characterize the interaction between FOXO3a and MMP-13 additional experiments were conducted. To ensure a sufficient activation of endogenous FOXO3a, NRFBs and NRVMs were cultured in normal culture media for 24 hours, with or without the addition of 50µM LY294002. LY294002 can selectively inhibit PI3k in the presence of growth factors, thereby abolishing the activating effect of PI3k on Akt activation. The inhibition of the PI3k-Akt signaling pathway potentiates FOXO3a activation. qRT-PCRs using MMP-13 TaqMan^{TM} probes were performed to observe the effect of endogenous FOXO3a on the MMP-13 mRNA expression levels in both cardiac fibroblasts and cardiomyocytes. As shown in Figure 10A-B, addition of 50µM LY294002 to the cultured NRFBs and NRVMs significantly up-regulates MMP-13 mRNA expression levels. Under these conditions, an MMP-13 mRNA expression increase of approximately 2-fold in NRFBs and 3-fold in NRVMs, respectively, was observed.

In another set of experiments, MMP-13 mRNA levels were determined in adult fibrobasts isolated from hearts of FOXO3a *wildtype* and *knockout* mice. Cardiac fibroblasts isolated from FOXO3a+/+ and FOXO3a-/- mice were cultured and grown under conditions of serum starvation to activate FOXO3a. In line with our previous results, MMP-13 mRNA expression was significantly decreased in FOXO3a-/- mice compared to *wildtype* littermates (Figure 10C).

Moreover, MMP-13 protein was quantified in NRVM cell lysates by western blotting to evaluate protein expression under normal growth conditions and serum starvation. Matrix metalloproteinases are secreted as pro-peptides, in which the catalytic domain is protected by the cysteine-Zn interaction. For MMPs activation to occur, the NH2-terminal sequence of the peptide domain is cleaved, resulting in exposure of the Zn-binding site of the catalytic domain. Therefore, when analyzing protein expression, a pro form (inactive form), an intermediate one and an active form of the MMPs can be detected. As shown on Figure 10D, serum starvation led to inactivation of the growth factor/PI3k/Akt signaling axis resulting in dephosphorylation (i.e. activation) of FOXO3a on a threonine 32 residue. MMP-13 pro form and intermediate form protein expression positively correlated with activated FOXO3a levels under conditions of serum starvation.

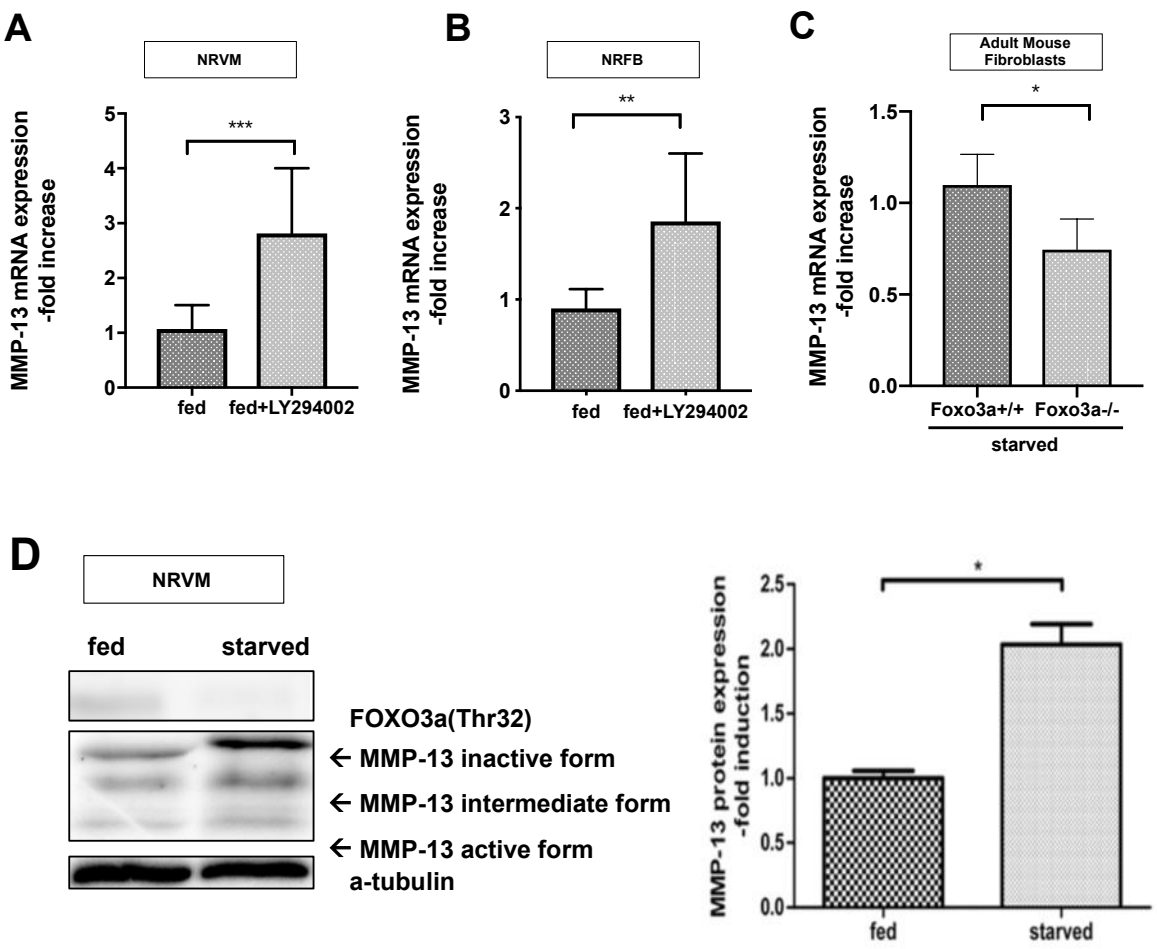

Figure 10: Endogenous FOXO3a up-regulates MMP-13 mRNA expression. A) NRVMs and B) NRFBs were cultured in growth media with or without a selective PI3k inhibitor (50µM LY294002). PI3k inhibition blocks Akt activation. Therefore, active (i.e., de-phosphorylated) FOXO3a can translocate to the nucleus and up-regulate target genes. The bar graph indicates three independent experiments performed in triplicates for each cell type expressed as Mean ± SE (**p<0,01, ***p<0,001). C) Cardiac fibroblasts from wildtype and FOXO3a-/- mice were cultured ex vivo. Under conditions of serum deprivation MMP-13 expression was determined. The bar graph illustrates MMP-13 mRNA expression as Mean±SE (*p<0.05). D) NRVMs were grown in growth media or serum starved for 24 hours and MMP-13 protein expression was assessed through western blotting. MMP-13 protein expression of the pro and intermediate form is significantly higher in serum starved NRVMs. The graph indicates the assessment of the immunoblots of three independent experiments in triplicates for the active form. A representative Immunoblot is shown.

Taken together, our data indicate that activation of FOXO3a leads to up-regulation of MMP-13 mRNA expression in both NRFB and NRVM as well as up-regulation of the pro and intermediate forms of MMP-13 protein expression in NRVM.

Endogenous and exogenous FOXO3a increases collagenolytic activity in NRFB

MMPs are proteins that degrade most constituents of the extracellular matrix. Therefore, to further investigate the functional effect of FOXO3a on the collagenolytic activity of NRFB, a collagenase assay was performed. In this assay, fluorescein labeled DQ collagen Type I serves as substrate for the collagenase. The DQ collagen Type I is degraded by MMP-13 collagenolytic activity resulting in release of fluorescent peptides. The collected supernatant from cells cultured in the presence ("fed") or the absence ("starved") of growth factors was employed in the assay. As shown in Figure 11B, FOXO3a activation led to a significant increase in collagenase activity ($p<0.01$). Moreover, transduction with AdV5-CMV-TM-FOXO3a for 24 hours significantly enhanced collagenase activity compared to transduction with a control vector (Figure 11A).

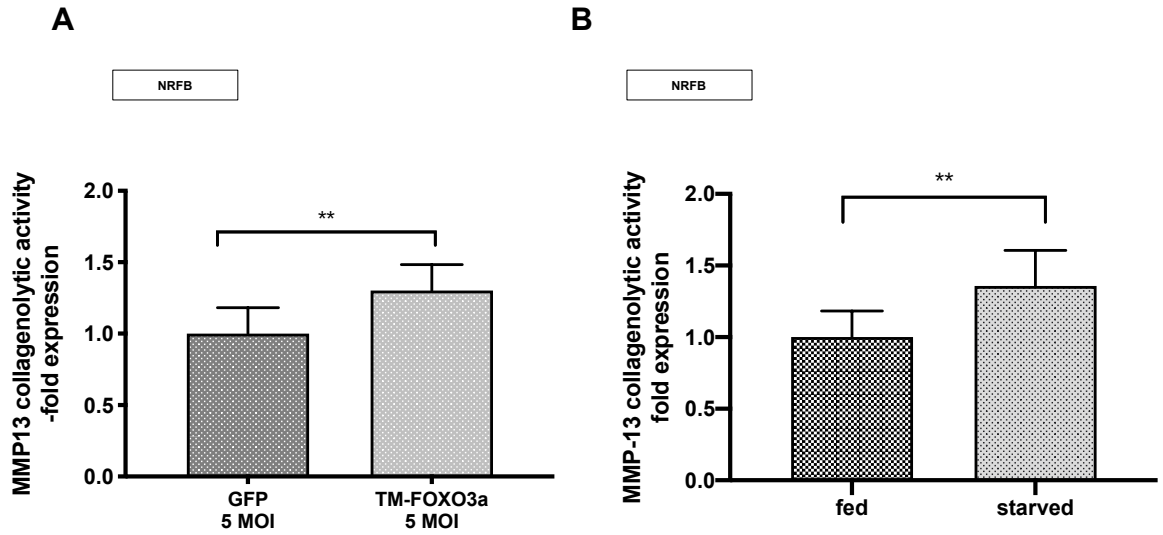

Figure 11: Endogenous and exogenous FOXO3a results in a higher collagenolytic activity in NRFBs. A) NRFBs transduced with either AdV5-CMV-GFP or AdV5-CMV-TM-FOXO3a for 24 hours. Cell lysates were used to assay the collagenolytic activity. Data are presented as Mean±SE for three independent experiments performed in triplicates in each group (*$p<0.05$, **$p<0.01$). B) NRFBs were cultured in growth media or starved for 24 hours and collagenolytic activity was assayed in cell lysates. Data are presented as Mean±SE for three independent experiments performed in triplicates (**$p<0.01$).

FOXO3a binds to and trans-activates the MMP-13 promotor region.

Endogenous and exogenous FOXO3a was shown to up-regulate MMP-13 expression at transcriptional and translational levels in NRVMs (Figure 9 B-C and 10). FOXO3a is a transcription factor that recognizes specific DNA sequences. Two conserved sequences are recognized by all FOXO proteins: the 5'-GTAAA(T/C)AA-3' sequence, known as the DAF-16 family member binding element (DBE), and the 5'-(C/A)(A/C)AAA(C/T)AA-3' sequence, presently known as the insulin-response element (IRE). FOXO3a binding sites for the core sequence are present in the MMP-13 promoter region. Therefore, our observations of increased MMP-13 mRNA and MMP-13 protein expression, following FOXO3a activation, could derive from direct binding of the transcription factor to the MMP-13 promoter region rather than mediated by other FOXO3a responder genes. In order to investigate a direct binding of FOXO3a on the MMP-13 promoter region, whole cell lysates of neonatal rat cardiomyocytes were analyzed performing a ChIP assay. Initially, the genomic DNA-Input amount for the ChIP showed no difference between cells cultured in normal medium when compared to those grown under serum starvation conditions. The same could be confirmed for transduced cells with AdV5-CMV-GFP or AdV5-CMV-TM-FOXO3a. This indicates a homogenous distribution of similarly sonicated DNA fragments between the two experimental groups of both experiments. A further amount of Control non-immunoprecipitated-DNA was used to identify FOXO3a antibody affinity to the cross-linked protein-DNA complexes. Figure 12B indicates that the FOXO3a antibody used for the immunoprecipitation possesses a high specificity when binding the transcription factor. After performing FOXO3a immunoprecipitation, all resulting FOXO3a-DNA complexes were isolated. DNA from these complexes was extracted and RT-PCR was performed to detect differences in the MMP-13 promoter presence. As shown in figure 12A a higher amount of MMP-13 promoter was extracted after immunoprecipitation from cells cultured under serum starvation conditions rather than from those cultured in normal growth media (presence of growth factors). Therefore, direct binding of FOXO3a to the MMP-13 promoter was dependent on FOXO3a activation status. Serum starvation associated with FOXO3a dephosphorylation led to an increased FOXO3a binding when compared to control cells incubated with growth media containing growth factors. In accordance with these data,

transduction of NRVM with a constitutively active FOXO3a led to detection of a higher amount of MMP-13 promoter region, indicating direct binding of the activated transcription factor to the promoter of the MMP-13 gene in neonatal rat cardiomyocytes (Figure 12B).
Taken altogether, our data indicate an ability of activated FOXO3a to bind to its target sequence in the MMP-13 promoter.

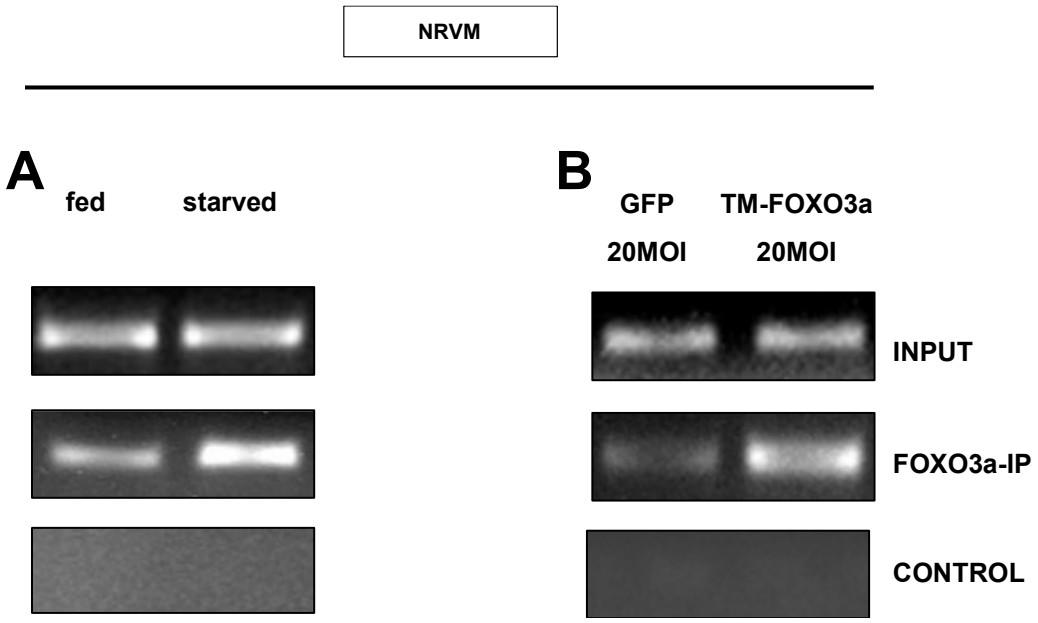

Figure 12: NRVMs endogenous and exogenous FOXO3a binds to the MMP-13 promoter. A) NRVMs were fed or serum starved or B) transduced with AdV5-CMV-TM-FOXO3a or AdV5-CMV-GFP and ChIP assay was performed. Direct binding of FOXO3a to the MMP-13 promoter is dependent on FOXO3a activation status. Data shown for three independent experiments performed in triplicates.

Endogenous and exogenous FOXO3a trans-activates MMP-13 promoter upon binding

As shown in Figure 12A and B, endogenous and exogenous FOXO3a can bind the MMP-13 promoter region. The interaction between transcription factors and DNA is complex. Part of this interaction are various cofactors such as activators and repressors that influence the typology, the nature and, most importantly, the outcome of this interaction.

To verify that FOXO3a indeed effectively stimulates the transcription of the MMP-13 gene by trans activating its promoter, a renilla luciferase assay was performed in NRVMs.

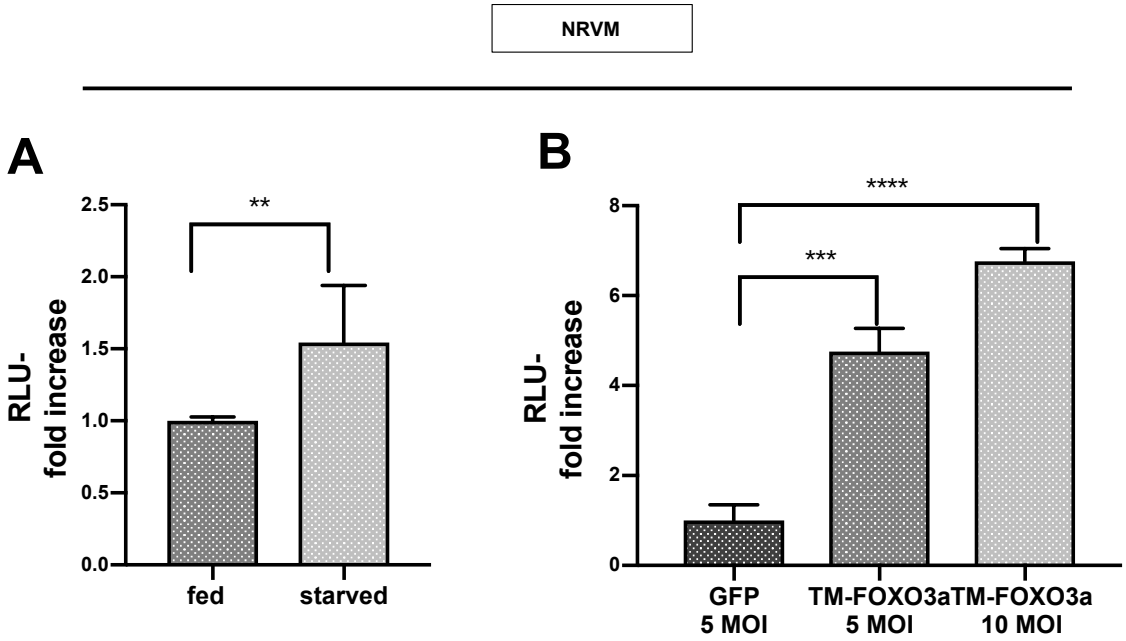

Figure 13: NRVMs exogenous and endogenous FOXO3a trans-activates the MMP-13 promoter. NRVMs were either serum starved overnight or transduced with AdV5-CMV-TM-FOXO3a overnight. Transfection with MMP-13 luciferase promoter constructs followed for four hours. Luminescence was measured. A) Endogenous FOXO3a activated by serum starvation. B) Bar graph indicating transactivation of the MMP-13 promoter following FOXO3a gene transfer. Data are presented as Mean±SE for three independent experiments performed in triplicates (****$p<0.01$).

After activation of FOXO3a in NRVMs by either serum starvation or transduction with AdV5-CMV-TM-FOXO3a overnight, cells were transfected with MMP-13 luciferase promoter constructs. Significantly, the MMP-13 promoter activity was approximately increased 1,5-fold in serum starved cells compared to cells cultured in medium containing growth factors (Figure 13A). In line with these observations, gene transfer of constitutively active FOXO3a led to a dose-dependent significance, i.e. an approximately 4,5-7-fold increase in MMP-13 promoter activity depending on the multiplicity of infection (MOI) used (Figure 13B).

Taken together, our results demonstrate that FOXO3a can directly bind to the MMP-13 promoter region and transactivate it, resulting in an up-regulation of MMP-13 mRNA and protein expression.

FOXO3a activation in *in vivo* models is associated with MMP-13 up-regulation

The *in vitro* experiments determined an up-regulation of MMP13 mRNA and protein expression by FOXO3a. Increased MMP-13 expression was associated with enhanced collagenolytic activity in a collagenase assay. The microcellular environment in the living organism is complex due to interaction between different signaling pathways, and therefore it is difficult to reproduce in *in vitro* experiments. In order to corroborate the *in vitro* findings and to assess whether a modulatory effect of FOXO3a on MMP-13 expression was also present *in vivo*, FOXO3a-MMP-13 interactions were investigated in several *in vivo* injury models.

FOXO3a regulates MMP-13 in a CVB3 myocarditis model

FOXO3a activation has been shown to be stress dependent. Injury stimuli create stressful cellular conditions that modulate the activity of the PI3k/Akt axis which in turn controls the activation status and consequently the functional activity of FOXO3a. Inflammation is characterized by increased redox stress, a potent activator of FOXO3a. In order to further characterize the regulation of MMP-13 by FOXO3a in inflammation, CVB3 myocarditis was induced in FVB mice. As shown in Figure 14, control *wildtype* mice and their control FOXO3a-/- littermates did not show a significant difference in MMP-13 expression. This observation can be explained by redundant gene function of other forkhead factors, such as FOXO1 and FOXO4. However, following CVB3 infection, MMP-13 mRNA expression was significantly higher in *knockout* mice compared to the *wildtype* littermates. This indicates that there are other regulators that influence MMP-13 mRNA expression in mice with an FVB genetic background in a model of CVB3-induced myocarditis, i.e., a different immune response.

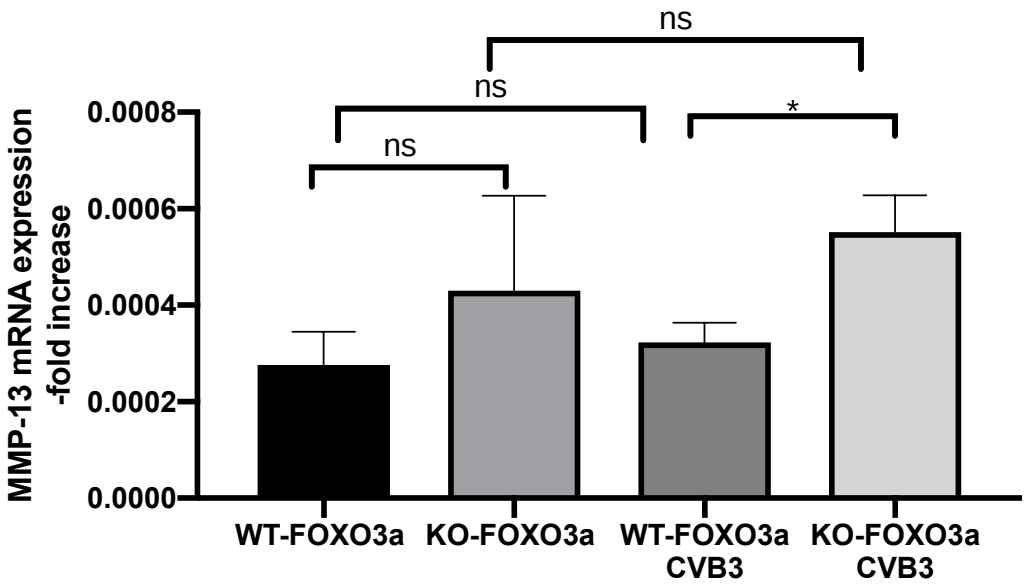

Figure 14: mRNA expression of MMP-13 is higher in FOXO3a *knockout* mice. MMP-13 mRNA expression is shown for the two groups of animals. FVB mice were infected with CVB3 virus and MMP-13 mRNA levels were assessed. The graph indicates levels of MMP-13 7 days after induction of myocarditis. Data are presented as Mean±SE for at least three animals for each group (*p<0.05).

FOXO3a regulates MMP-13 in a myocardial infarction model

FOXO3a is activated in stress conditions. Ischemic injury occurring in the early phases of a myocardial infarction is associated with the generation of oxygen reactive species a redox disbalance in the cell due to the reduction of oxygen and nutrients available to the cell. This disequilibrium with repercussion into ATP production and shift towards the accumulation of AMP in the cell activates AMPK, an up-stream regulator of FOXO3a. AMPK phosphorylates and activates FOXO3a in six different sites (31). Therefore, an MI *in vivo* model was chosen to investigate the effect of a ROS-induced FOXO3a activation on the MMP-13 mRNA and protein expression.

FOXO3a activation in the MI model in *wildtype* animals was confirmed performing a ChIP assay as shown in Figure 15A. After performing the FOXO3a immunoprecipitation step, FOXO3a-MMP-13 promoter region complexes were de cross-linked and RT-PCR was performed to assess the potential difference in MMP-13 promoter region presence three days after the sham procedure or the coronary artery ligation were performed. An increased level of MMP-13 promoter was identified three days following coronary artery ligation in mice at the infarction site and scar tissue. Increased FOXO3a activity within the scar and infarcted area was accompanied by significantly increased MMP-13 mRNA

expression as shown in Figure 15B. There was a significant difference of MMP-13 mRNA levels between the infarction site and the scar tissue, where MMP-13 was present at higher levels. In order to investigate whether there was a connection between the activation of transcriptional mechanisms and translational ones and to also assess whether FOXO3a has a direct effect on MMP-13 protein expression at the infarction site, protein quantification of MMP-13 at the infarction site was performed. MMP-13 protein levels were significantly lower in *knockout* mice compared to the *wildtype* ones (Figure 16A). The graph indicates immunoblot assessment of protein quantification (Figure 16B).

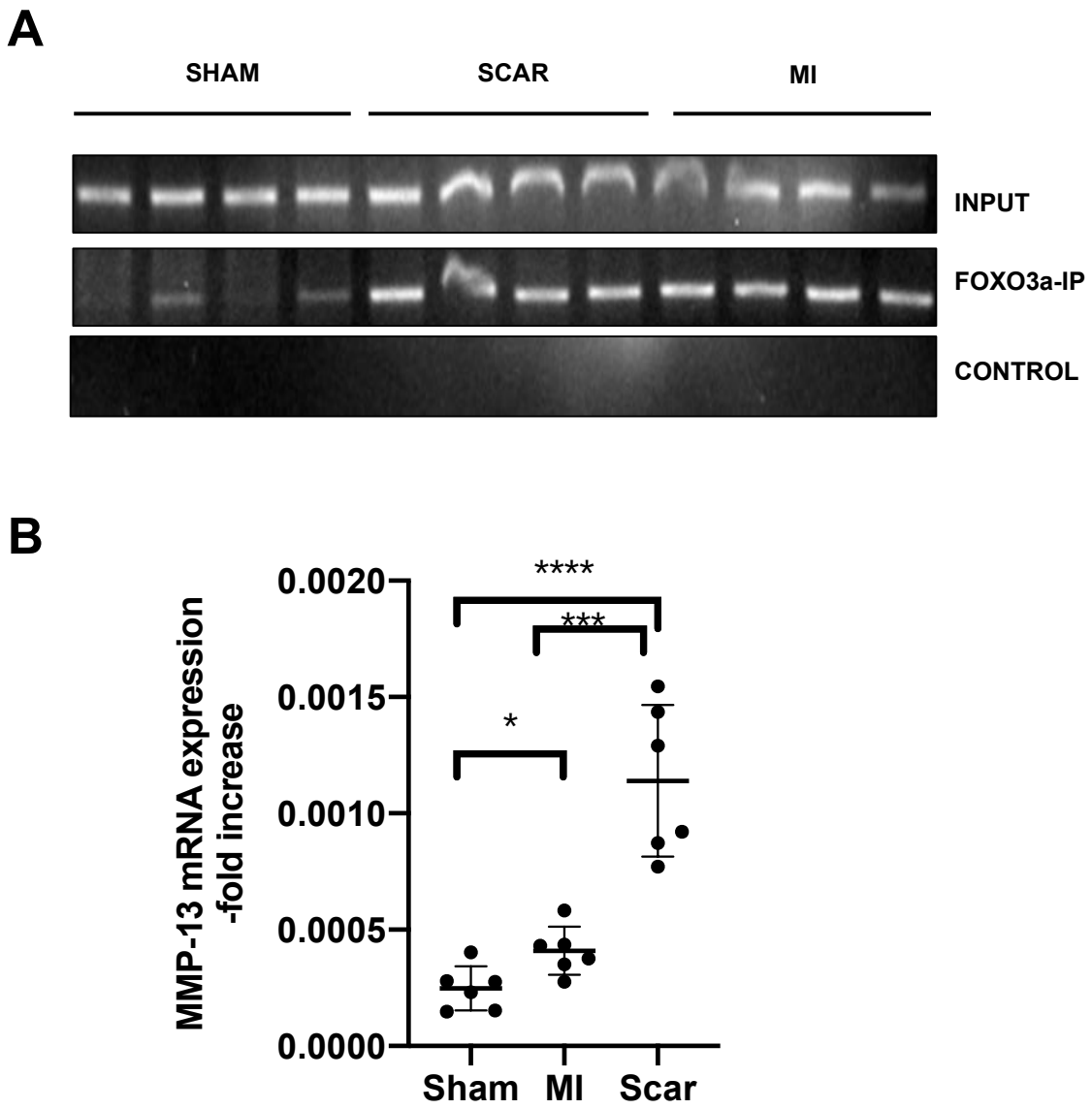

Figure 15: FOXO3a activation in *wildtype* mice increases MMP-13 expression at the infarction site and scar tissue. A) The ChIP assay shows activation of FOXO3a and binding of the transcription factor to the MMP-13 promoter in the infarcted area. B) FOXO3a activation three days post-MI is associated with up-regulation of MMP-13. B) The bar graph indicates Mean±SE for five animals in each group (*p<0,05, ****p<0.01.).

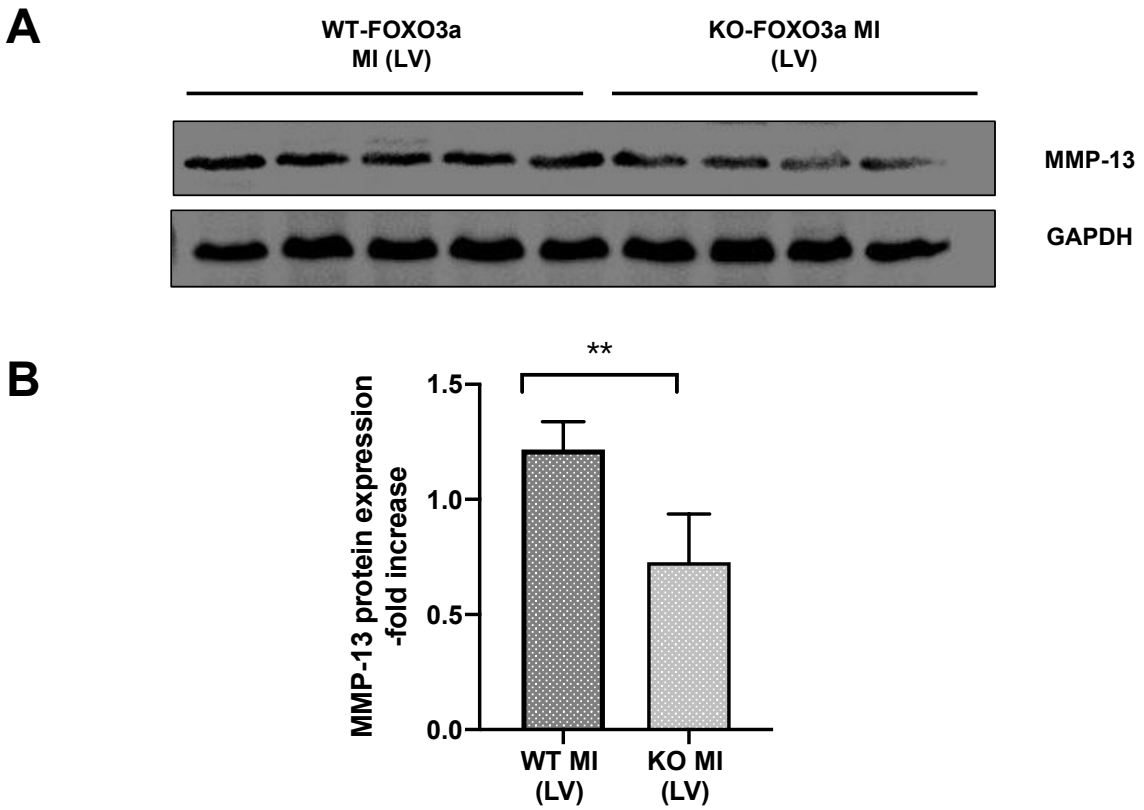

Figure 16: MMP-13 protein expression results decreased in *knockout* mice at the MI site. A) MMP-13 protein expression in *wildtype* and *knockout* mice at the myocardial infarction site. B) Immunoblots assessment normalized to GAPDH through Image J showing a significant decrease in MMP-13 expression in *knockout* mice in five *wildtype* mice and four *knockout* mice (*p<0,05, **p<0,01).

Taken together, our data implicate FOXO3a activated by inflammatory/redox stress in the up-regulation of MMP-13 mRNA expression in myocardial ischemia but not in myocarditis at peak inflammation.

Discussion

The present study investigates the effects of FOXO3a on MMP-13 expression in cardiac matrix remodeling. Initially, FOXO3a effects on mRNA or protein levels on important ECM regulators were assessed. FOXO3a did not significantly modulate mRNA levels of MMP-3, MMP-9, TIMP-1 or TIMP-2. Moreover, FOXO3a did not affect protein levels of MMP-1 and TIMP-4. In contrast to other ECM regulators, MMP-13 mRNA and protein were subject to FOXO3a regulation. MMP-13 mRNA levels increased in a dose-dependent manner following transduction of cardiac NRFB and NRVM with replication defective adenoviral vectors overexpressing constitutively–active FOXO3a (TM-FOXO3a) *in vitro*. Moreover, MMP-13 protein levels were also up-regulated in a dose-dependent manner in NRVM transduced with adenoviral vectors overexpressing a constitutively active FOXO3a (TM-FOXO3a). Furthermore, these results could be corroborated with endogenous cardiac cells lacking FOXO3a that showed diminished levels of MMP-13 expression. Activation of FOXO3a up-regulated, while inhibition of FOXO3a by phosphorylation of the Akt consensus phosphorylation sites diminished MMP-13 mRNA as well as protein expression *in vitro*. Furthermore, FOXO3a was found to directly bind and trans-activate the MMP-13 promoter in cardiomyocytes. Additionally, FOXO3a also increased MMP-13 collagenolytic activity in fibroblasts, leading to increased cleavage of collagen I. In murine models of cardiac injury, activation of FOXO3a was determined. In the *in vivo* models, FOXO3a *knockout* in murine myocarditis did not affect MMP-13 expression, indicating that FOXO3a activity is not the main regulator of MMP-13 in a CVB3-induced myocarditis model. FOXO3a did up-regulate cardiac MMP-13 expression in a murine model of myocardial infarction and FOXO3a activity correlated with higher expression of MMP-13 protein levels at the infarction site. Therefore, further identification of the role of forkhead transcription factors in cardiac pathology is warranted.

FOXO3a and cardiac remodeling

Cardiac remodeling plays an important role in many cardiac diseases such as volume overload (mitral regurgitation), pressure overload (aortic stenosis, hypertension), inflammation (myocarditis), genetical disorders (DCM) or ischemia (myocardial

infarction). Long-term cardiac remodeling correlates with progressive LV dysfunction and it is associated with a higher morbidity and mortality (6).
Following myocardial injury, the initial inflammatory response and the complex activation of a myriad of signaling pathways are intended to orchestrate a healing process at the injured site. Cardiomyocyte hypertrophy and diffuse fibrosis are the most characteristic patterns of this cardiac remodeling process. At present, very little is known about the role and targets of FOXO3a in these typical patterns of cardiac remodeling.

FOXO3a and cardiomyocyte hypertrophy in cardiac remodeling

FOXO3a, as a transcription factor, has multiple targets and regulates different cellular processes in a cell-type specific manner. Its role in cardiac remodeling so far has been attributed to its ability to counteract hypertrophy in skeletal muscle and cardiac myocytes (38) (37). Autophagy- and proteasome-mediated proteolysis decrease cardiomyocyte size through a catabolic response leading to cardiac atrophy. Atg genes are a set of genes that encode for proteins that coordinate autophagy. FOXO3a controls expression of some of these atg genes. FOXO3a induces the expression of several autophagy genes, which are associated with different phases of autophagy, including LC3b (Map1lc3b), Gabarapl1, Pi3kIII, Ulk2, Atg12l, Beclin1, Atg4b, and Bnip3 (105).

Our group has shown that insulin and stretch-induced hypertrophy can be reversed through FOXO3a gene overexpression (37). Moreover, cardiac overexpression of FOXO3a leads to atrophy in mouse hearts in vivo. According to this study, FOXO3a activates an atrogenic program, up-regulating the ubiquitin ligases atrogin-1 and MuRF-1, which results in a catabolic state and activation of protein degradation by the proteasome pathway leading to a net loss of cardiac mass. Taken together, these data characterize FOXO3a as an important transcription factor regulating myocardial remodeling. In this regard, Ni and colleagues have reported that the expression of FOXO3a in cardiomyocytes counteracts hypertrophy by attenuating the calcineurin/NFAT pathway, which is known to lead to hypertrophy (106). In the same study by Ni et al., it was shown that both basal and hypertrophic agonist-induced expression of MCIP1.4, a direct downstream target of the calcineurin/NFAT pathway,

were down-regulated due to FOXO3a expression (106). Moreover, a study from Galasso et al. performed in human cardiac tissue from healthy patients and patients with heart failure, also determined reduced activity of Akt and activation of FOXO3a as well as induction of atrogin-1 (107). These data suggest that FOXO3a-atrogin-1 up-regulation in heart failure correlates with an impairment of cardiac function. However, the study presents no follow-up data.
Löbel et al. have identified that the longevity-associated FOXO3a SNP is protective in the chronic phase of myocarditis (108).

Moreover, FOXO3a is important in ROS detoxification (84). It transcriptionally up-regulates the catalase and manganese superoxide dismutase (MnSOD) genes, both encoding antioxidative enzymes (109) (110). In this regard, several studies have shown that the anti-oxidative effect of FOXO3a counteracts cardiomyocyte hypertrophy, thereby influencing cardiac remodeling and cardiac function. Sirt3 prevents cardiac hypertrophy through FOXO3a-dependent MnSOD and catalase up-regulation (111). In addition, in a study by Tan et al., the inhibitory effect of FOXO3a on cardiomyocyte hypertrophy has also been associated to its ability to transcriptionally up-regulate catalase (112). The same study also showed that FOXO3a could also down-regulate myocardin, a downstream mediator of ROS in conveying the hypertrophic signal of insulin or IGF-1 signaling pathways (112). Taken together, these data show the relevance of the anti-hypertrophic effects of FOXO3a on cardiac remodeling either by directly targeting atrophy inducing genes or inhibiting expression of pro hypertrophic downstream targets of ROS-activated signaling pathways.

Supporting the results of the present study, Yu et al. have recently investigated the role of FOXO3a in vascular remodeling related to atherosclerosis (43). This group of investigators showed that endogenous and exogenous levels of FOXO3a up-regulate MMP-13 at an mRNA and protein level in vascular smooth muscle cells (VSMCs). Furthermore, they show that FOXO3a directly binds and trans-activates the MMP-13 promoter region. In addition, they identify that FOXO3a-induced apoptosis was partially attributed to MMP-13. The data of Yu et al. together with this study indicate an important role of FOXO3a-MMP-13 signaling in cardiovascular remodeling.
The present research was able to determine a FOXO3a-induced increase of MMP-13 levels after FOXO3a overexpression as well as after abrogating the inhibitory effect

from the PI3k/Akt signaling pathway, respectively. FOXO3a is a downstream target of the PI3k/Akt signaling. Growth factors and cytokines activate Akt, which phosphorylates and inhibits FOXO3a. The present study conducted in cardiomyocytes and fibroblasts is in line with the study from Yu et al. who investigated the effects of FOXO3a on MMP-13 in vascular smooth muscle cells. Moreover, the transduction of human umbilical endothelial cells (HUVECs) with replication defective adenoviral vectors overexpressing constitutively–active FOXO3a (TM-FOXO3a) resulted in MMP-3 up-regulation and a decrease of TIMP-1 (113). Furthermore, FOXO3a can also up-regulate MMP-10 in endothelial cells (114).

As illustrated above, FOXO3a acts ubiquitously in the cardiovascular system in a cell and context specific manner, and stimulates MMP gene expression in cardiomyocytes, cardiac fibroblasts, endothelial cells and vascular smooth muscle cells. The above-mentioned studies implicate FOXO3a activity in cardiac and vascular remodeling. By targeting MMP genes in different cell types upon cardiac injury, FOXO3a deserves particular attention as an important regulator of cardiovascular remodeling.

FOXO3a and cardiac fibrosis in cardiac remodeling

As previously stated, cardiac fibrosis is one of the characteristic patterns of cardiac remodeling with distinctive pathological implications. Typically, following injury, fibroblasts transform into myofibroblasts by acquiring an increased secretory profile. The deposition of collagen is intended to replace the lost or damaged tissue. In physiological wound healing, this deposition is limited in time and space. An abnormal activity of these cells causes an aberrant accumulation and deposition of collagen leading to cardiac fibrosis.

Diffuse cardiac fibrosis negatively impacts cardiac function in a setting of ongoing cardiac remodeling. It affects the electrical conduction system leading to arrhythmias, it impedes access to necessary nutrients causing a global state of ischemia and it interferes with cardiomyocyte contractile function resulting in ventricular dysfunction (115).

Cardiac fibrosis causes rhythm disturbances such as circuits that block or slow signal conduction. Recent studies show that fibrosis may also affect the potentials after depolarization that lead to atrial and ventricular fibrillation (115). The basal membrane

is crucial in the diffusion and transport of nutrients from the circulation to the cardiomyocyte. Perivascular fibrosis of the coronary arteries modifies the composition of the basal membrane, rendering it less permeable to oxygen and nutrients resulting in a state of ischemia and nutrient deprivation that impairs cellular processes and induces metabolic responses that worsen myocardial function. The abnormal deposition of collagen in myocardial scarring is associated with qualitative modifications of collagen fibers. Abnormally, cross-linked collagen is present and it intervenes with myocyte orientation and survival causing an impairment of the systolic and diastolic function. Since cardiomyocytes lack regenerative properties, necrotic tissue is replaced by a fibrotic scar. There are 3 overlapping phases that can be identified in the fibrotic response: the inflammatory phase, the proliferative phase and the scar formation and the maturation phase. During the inflammatory response, enhanced chemotaxis of inflammatory cells is present. Matrix degradation renders the injured site accessible to immune cells. A provisional matrix composed of fibrin and fibronectin is formed for the immune response to take place. Locally, the inflammation is stopped before passing to the proliferative phase. Characteristically, there is a deposition and accumulation of collagen for the scar formation. Myofibroblasts are the cells in charge of collagen deposition. Resident fibroblasts acquire new characteristics that consist mainly of a higher secretory profile and the ability to synthesize contractile fibers, thus transdifferentiating into myofibroblasts. The scar maturation is intended as the shaping of the scar based on the tensile forces during systolic and diastolic function. Myofibroblasts disappear due to the lack of growth factors. In this regard, angiogenesis is physiologically required during wound healing. Myocardial angiogenesis is strictly coordinated by angiogenic growth factors such as VEGF, FGF, PDGF and angiopoietin-1 and -2. Physiological cardiac hypertrophy is associated with a proportional new formation of blood vessels to correspond to the increased demand for oxygen and nutrients. Short term Akt1 stimulation leads to physiological increase in cardiomyocyte cell size and at the same time up-regulates VEGF. However, long term activation of the PI3K/Akt signaling pathway has a negative impact on cardiac function. In a study by Shiojima et al., Akt activation caused maladaptive cell hypertrophy and increased scar formation (116). This could indicate that long term suppression of FOXO3a target gene transcription due to protracted Akt activation over time has a deleterious impact on cardiac remodeling.

In this regard, as mentioned above, Potente et al. have demonstrated that the FOXO transcription factors FOXO1 and FOXO3a, but not FOXO4, are critical regulators of endothelial sprout formation and migration in vitro. In this study, HUVECs were transfected with FOXO3a siRNA and gene profiling was performed. FOXO3a was found to have anti-angiogenic effects. FOXO3a silencing up regulated eNOS, essential for neo angiogenesis. Amongst other genes, MMP-10 mRNA was repressed under FOXO3a siRNA conditions in this cell type (114).
Altogether, these data indicate that FOXO3a might coordinately regulate cell size and angiogenesis. By inducing signaling pathways that favor ECM degradation, confirmed through the present research, atrophy in cardiomyocytes (37) (38) and inhibiting angiogenesis (114), FOXO3a may equilibrate the cardiac muscle cell size and blood supply , thereby facilitating diffusion of nutrients and oxygen to the myocardium. FOXO3a involvement in cardiac remodeling appears on a multilevel scale, influencing and coordinating different physiological processes.

In progressive fibrotic disorders there is an excessive activation and proliferation of fibroblasts, which are also typically resistant to apoptosis. Thus, inducing apoptosis of activated fibroblasts or inducing ECM degradation may prove effective in progressive fibrotic disorders.

FOXO3a can reduce the proliferation rate of fibroblasts by upregulating cell cycle inhibitors, including p21CIP1 and p27, leading to cycle arrest and playing an important role in this regard (117) (118). Furthermore, several studies have described the role of FOXO3a in fibroblast physiology. There are only few data describing its role in cardiac fibroblasts. In adult rat cardiac fibroblasts, FOXO3a regulates cell cycle progression by increasing p27kip1 expression, an inhibitor of cyclin dependent kinase, through an ERK1/2 dependent signaling pathway. In the heart of diabetic mice elevated collagen levels are associated with low levels of FOXO3a (119).

FOXO3a activity on MMP and TIMP expression has also been subject to recent research. MMPs are important factors in tissue repair and wound healing in response to injury. Depending on the extent and duration of myocardial ischemia, collagen damage could present early and in an extensive manner (120). Different studies have investigated the temporal and spatial distribution after ischemic injury.

MMP-1 collagenolytic activity has been identified one hour after myocardial infarction caused by artery ligation in rats, with a peak activity level at four hours and reidentification of its activity after 24 hours (121) In the present study, FOXO3a did not influence the MMP-1 protein levels in NRVM.

The time course of MMP-9 induction was investigated by Romanic et al., who demonstrated that MMP-9 was up-regulated within 24 hours of myocardial infarction and that this rise was accompanied by a reduction in the physiological inhibitor of MMP-9, TIMP-1 (122). The same study indicated that MMP-3 activity was induced 2 days after the myocardial infarction. However, FOXO3a did not significantly modulate mRNA levels of MMP-9, MMP-3 or TIMP-1.

A study conducted by Sawicki et al. in a canine model of ischemia/reperfusion injury, found that TIMP-4 levels were unchanged in the infarct zone. In contrast to TIMP-4, TIMP-2 was detected in both ischemic and non-ischemic tissue (123). There was no modulation of TIMP-2 and TIMP-4 levels in NRVM with FOXO3a overexpression.

In the present study, FOXO3a could up-regulate MMP-13 mRNA and protein levels. MMP-13 activity has been detected in the infarct and remote areas after ischemic injury. According to a review from Lindsey et Zamilpa, MMP-13 mRNA remains stable following MI through week 16 in the rat, however, a significant increase in MMP-13 enzyme activity is detected after Week One, peaks at Week Two and returns to baseline at Week Eight (124). According to the results of the research of Lindsey et Zamilpa, MMP-13 activity appears to be involved in the long-term remodeling of the left ventricle after injury. Long-term maladaptive remodeling pathways are associated, amongst others, with ROS formation. FOXO3a is activated under stress conditions, and its involvement in regulation of MMP-13 but not of other cardiac ECM regulators, indicates a potential important role of FOXO3a in this process.

All these data suggest that FOXO3a activation might be associated with decreased fibrosis, by regulating fibroblast proliferation, apoptosis sensitivity (125) and collagen degradation. This evidence adds to the multimodal spectrum of activities of FOXO3a in tissue remodeling.

FOXO3a and MMP-13 signaling pathways in cardiac remodeling

FOXO3a and MMP-13 in pathologies

Few studies show that the inhibition of FOXO3a is associated with a proliferative pathological fibroblast phenotype, which contributes to the development of fibrosis in different pathologies. However, whether FOXO3a has other targets that may influence fibrosis, e.g. ECM regulators, particularly in cardiac remodeling, remains unknown. FOXO3a has been implicated in different models of fibrosis such as idiopathic pulmonary disease, renal or liver fibrosis. Primary fibroblast cultures obtained from idiopathic pulmonary fibrosis (IPF) are characterized by their ability to elude the proliferation-suppressive properties of polymerized type I collagen. This ability involves the aberrant activation of the PI3K/Akt signaling pathway that inactivates FOXO3a, resulting in p27kip1 down-regulation and a decreased sensitivity to apoptosis. In a model of renal fibrosis induced by unilateral ureteral obstruction, accumulation of collagen and increased expression of α-SMA, characteristic of myofibroblasts, is associated with FOXO3a inactivation (126). Furthermore, in the liver, FOXO3a also regulates the proliferation and apoptosis of hepatic stellate cells (125).
In the heart, after tissue injury, fibroblasts differentiate into myofibroblasts, which tend to have a high secretory profile and be resistant to apoptosis (118). These cells produce high quantities of ECM proteins, mainly collagen, leading to fibrosis. FOXO3a activation can also modulate the sensitivity of the myofibroblasts to apoptosis by activating downstream targets, such as p27kip1, to induce a programmed cellular death (118). Supporting the results of the present work, Yu et al. implicate FOXO3a and MMP-13 in vascular remodeling, characteristic of atherosclerosis (43). Furthermore, reduced MMP-13 levels have been identified in patients with structural, functional, and clinical manifestations of hypertensive heart disease. In these patients, the decreased expression of MMP-13 was associated with reduced collagen turn-over and degradation leading to extracellular matrix accumulation (127).
The present study is the first to provide data on the effect of FOXO3a on cardiac remodeling and its regulation on MMP-13 and collagenolytic activity in neonatal rat cardiac fibroblasts and cardiomyocytes. Moreover, MMP-13 levels have been shown to

be present in the infarcted and remote area as far as eight weeks after ischemic injury (124).

In vitro, FOXO3a was associated with higher MMP-13 expression in both cell types. Furthermore, FOXO3a up-regulated the collagenolytic activity of NRFBs. The effect of FOXO3a on MMP-13 expression was assessed further in *in vivo* models of myocardial infarction (MI) and CVB3-induced myocarditis.
In MI, MMP-13 mRNA levels were assessed in *wildtype* mice in the infarct and scar areas. Three days post-MI, a ChIP assay showed an activation of FOXO3a and binding to the MMP-13 promoter in the infarct area as well as in the scar tissue in *wildtype* mice. There was a significant up-regulation of MMP-13 mRNA in both areas, with a higher expression in the scar tissue. Furthermore, MMP-13 protein levels were also assessed in the infarcted area in the present study. *Knockout* mice showed a reduced MMP-13 protein expression when compared to the *wildtype* ones. This indicates an important function of FOXO3a in MMP-13 protein synthesis. However, the MI model presents limitations. Only a correlation between activation of FOXO3a in *wildtype* but not *knockout* mice and MMP-13 mRNA expression in the infarct and scar area could be established. Furthermore, no ChIP assay for the FOXO3a activation in the *knockout* mice was performed.

In a second *in vivo* model, MMP-13 expression was determined in *wildtype* and FOXO3a deficient mice following CVB3 virus infection. There was no significant difference in MMP-13 mRNA expression in *wildtype* or *knockout* mice prior to the induction of myocarditis. However, there was a significantly higher expression of MMP-13 mRNA in *knockout* mice compared to the *wildtype* ones seven days after CVB3 infection. An increase in MMP-13 mRNA expression seven days after the induction of myocarditis through a CVB3 infection in mice, was also shown in a study by Becher et al., corroborating our results (80). The increased MMP-13 mRNA expression in *knockout* mice seven days after CVB3 infection indicates a somewhat smaller role of FOXO3a on MMP-13 mRNA up-regulation in this model. The observed discrepancy might be due to different genetic backgrounds of mice (FVB mice in CVB3 myocarditis, C57BL/6J in MI) or a differential temporal expression of MMP-13 or differential activation of complex signaling pathways in this specific animal model of cardiac injury.

Myocarditis is a cause of death amongst children and young adults. The most common cause of myocarditis is a CVB3 infection. There is a need for more comprehensive studies regarding the role of FOXO3a in myocarditis. However, a study by Löbel et al. has provided some interesting and important insights. This research showed that FOXO3a regulates the activity of NK cells, consequently playing an important role in innate immune response to myocarditis. FOXO3a-/- mice showed a bigger inflammatory infiltrate compared to their *wildtype* littermates. Furthermore, the longevity-associated FOXO3a SNP (rs12212067) was shown to be protective in the chronic rather than acute phase of myocarditis (108).
Therefore, further studies are warranted for a better characterization of FOXO3a's activity and effect in murine CVB3-induced myocarditis models.

Modification of extracellular matrix content is believed to be associated with phenotypical, functional and clinical outcomes. In pressure overload states such as arterial hypertension, left ventricular hypertrophy is characterized by increased fibrillar collagen content, altered fibrillar collagen geometry and an imbalance in the collagen I/collagen III ratio favoring collagen I deposition (2). At the same time, FOXO3a is inactivated in pressure overload (37) Regression of cardiac myocyte size and therefore, left ventricular hypertrophy, is mediated by FOXO3a activation (38) (37) and requires appropriate remodeling of the ECM, including degradation and turnover of ECM components as well as alterations in cardiomyocyte–matrix interactions. Thus, FOXO3a by up-regulating MMP-13 mRNA expression and increasing the collagenolytic activity in cardiac fibroblasts might coordinate regression of cardiac myocyte hypertrophy and increased collagen degradation which would result in improvement of cardiac function
The present work aimed at further characterizing the effect of FOXO3a on cardiac remodeling by analyzing its role on ECM regulators. In a panel with the most important ECM regulators, FOXO3a was found to modulate MMP-13 levels in NRFBs and NRVMs *in vitro*. The myocardial infarction in vivo model of the present study showed a decreased MMP-13 expression in FOXO3a *knockout* mice. However, the same effect was not identified in a CVB3-myocarditis *in vivo* model. As discussed above, this difference in the results could be due to a differential temporal expression or differential activation signaling pathway of MMP-13 expression in the absence of FOXO3a in a CVB3-myocarditis model or the genetic background of the mice used for the experiments.

Taken together, FOXO3a coordinately regulates cardiac myocyte size as well as cell-matrix-remodeling following myocardial infarction in the infarcted area and scar tissue by up-regulating MMP-13 expression. However, the role of FOXO3a on MMP-13 expression is somewhat reduced in a CVB3-induced myocarditis model. Therefore, further identification of the role of forkhead transcription factors in cardiac pathology is warranted.

Summary and conclusions

Cardiac remodeling encompasses the entity of responsive mechanisms activated upon cardiac injury, namely cardiac hypertrophy and fibrosis. Adaptive and maladaptive signaling pathways have been the focus of recent research in an attempt to elucidate new potential therapeutical targets in cardiac remodeling.

In cardiac remodeling, the role of FOXO3a has been attributed to its ability to up-regulate genes such as atrogenes, including the ubiquitin ligases atrogin-1 and MuRF-1, which result in a catabolic state via proteolysis leading to a net loss of cardiac myocyte mass (38) (37).

Since a change in cardiomyocyte size should be associated with a change in the extracellular matrix interactions of the cardiomyocyte, we hypothesized that FOXO3a coordinately regulates matricellular and myocardial remodeling.

The present study investigated the role of FOXO3a on cardiac matrix remodeling by determining its effects on the expression of several regulators of matrix turnover in cardiomyocytes and cardiac fibroblasts.
Here, FOXO3a was found to increase the expression of MMP-13 expression in both cardiac fibroblasts and cardiomyocytes by performing experiments *in vitro*. Overexpression of FOXO3a employing a replication defective adenoviral vector encoding for a constitutively-active FOXO3a led to an in increase in MMP-13 expression. These results were corroborated by endogenous FOXO3a, when a selective PI3k inhibitor was used to block the Akt-mediated inactivation of FOXO3a. Furthermore, overexpression of FOXO3a in cardiac fibroblasts led to an increase in collagenolytic activity. Based upon these results, the interaction between FOXO3a and MMP-13 was further investigated. Through a ChIP assay and a renilla luciferase assay, it was confirmed that FOXO3a can directly bind and trans-activate the promoter region of the MMP-13 gene. However, *in vivo* studies partially corroborated the results from the *in vitro* experiments. In this study, two murine *in vivo* cardiac injury models were used: a CVB3-induced myocarditis model and a myocardial infarction model. In these models FOXO3a is activated due to the stress conditions related to these injuries. MMP-13 was

up-regulated in mice who underwent the LAD ligature procedure in the MI model compared to the mice who received the sham procedures. MMP-13 protein expression was decreased in *knockout* mice at the infarction site, when compared to their *wildtype* littermates. The results are supported by the data provided by the work of Yu et al. They were also able to show a FOXO3a-dependent up-regulation of MMP-13 in vascular smooth muscle cells (VSMCs) in an atherosclerotic pathological setting (43). In the CVB3-induced myocarditis model, FOXO3a *knockout* showed a significantly higher expression of MMP-13 mRNA levels when compared to their *wildtype* littermates. The observed discrepancy might be due to different genetic backgrounds of mice (FVB mice in CVB3 myocarditis, C57BL/6J in MI) or a differential temporal expression of MMP-13 or differential activation of complex signaling pathways in this specific animal model of cardiac injury. In the present CVB3-myocarditis model, MMP-13 up-regulation was identified in FOXO3a *knockout* mice. Therefore, MMP-13 expression in this model should be subject to different regulatory mechanisms other that the ones orchestrated by FOXO3a.

Taken together our data indicate that FOXO3a coordinatively regulates cardiac myocyte size as well as cell-matrix-remodeling by up-regulating MMP-13 expression.
These results are of particular clinical importance since cardiac remodeling represents the cellular and molecular mechanistic basis of left ventricular dysfunction, clinically manifested as heart failure.

By targeting cardiac hypertrophy and ROS levels, FOXO3a has cardio-protective effects. The present work showed an additional regulatory effect of FOXO3a on MMP-13 expression. Therefore, further identification of the role of forkhead transcription factors in cardiac pathology is warranted.

REFERENCES

1. Souders CA, Bowers SL, Baudino TA. Cardiac fibroblast: the renaissance cell. Circulation research. 2009;105(12):1164-76.

2. Spinale FG. Myocardial matrix remodeling and the matrix metalloproteinases: influence on cardiac form and function. Physiological reviews. 2007;87(4):1285-342.

3. Fraccarollo D, Galuppo P, Bauersachs J. Novel therapeutic approaches to post-infarction remodelling. Cardiovascular research. 2012;94(2):293-303.

4. Hochman JS, Bulkley BH. Expansion of acute myocardial infarction: an experimental study. Circulation. 1982;65(7):1446-50.

5. Pfeffer JM, Pfeffer MA, Braunwald E. Influence of chronic captopril therapy on the infarcted left ventricle of the rat. Circulation research. 1985;57(1):84-95.

6. Cohn JN, Ferrari R, Sharpe N. Cardiac remodeling--concepts and clinical implications: a consensus paper from an international forum on cardiac remodeling. Behalf of an International Forum on Cardiac Remodeling. Journal of the American College of Cardiology. 2000;35(3):569-82.

7. Grossman W, Jones D, McLaurin LP. Wall stress and patterns of hypertrophy in the human left ventricle. The Journal of clinical investigation. 1975;56(1):56-64.

8. Opie LH, Commerford PJ, Gersh BJ, Pfeffer MA. Controversies in ventricular remodelling. Lancet (London, England). 2006;367(9507):356-67.

9. Sugden PH. Mechanotransduction in cardiomyocyte hypertrophy. Circulation. 2001;103(10):1375-7.

10. Baines CP, Molkentin JD. STRESS signaling pathways that modulate cardiac myocyte apoptosis. Journal of molecular and cellular cardiology. 2005;38(1):47-62.

11. Kim HE, Dalal SS, Young E, Legato MJ, Weisfeldt ML, D'Armiento J. Disruption of the myocardial extracellular matrix leads to cardiac dysfunction. The Journal of clinical investigation. 2000;106(7):857-66.

12. Woodiwiss AJ, Tsotetsi OJ, Sprott S, Lancaster EJ, Mela T, Chung ES, Meyer TE, Norton GR. Reduction in myocardial collagen cross-linking parallels left ventricular dilatation in rat models of systolic chamber dysfunction. Circulation. 2001;103(1):155-60.

13. Weber KT, Pick R, Janicki JS, Gadodia G, Lakier JB. Inadequate collagen tethers in dilated cardiopathy. American heart journal. 1988;116(6 Pt 1):1641-6.

14. Rutschow S, Li J, Schultheiss HP, Pauschinger M. Myocardial proteases and matrix remodeling in inflammatory heart disease. Cardiovascular research. 2006;69(3):646-56.

15. Azevedo PS, Polegato BF, Minicucci MF, Paiva SA, Zornoff LA. Cardiac Remodeling: Concepts, Clinical Impact, Pathophysiological Mechanisms and Pharmacologic Treatment. Arquivos brasileiros de cardiologia. 2016;106(1):62-9.

16. Weigel D, Jackle H. Novel homeotic genes in Drosophila melanogaster. Biochemistry and cell biology = Biochimie et biologie cellulaire. 1989;67(8):393-6.

17. Weigel D, Jackle H. The fork head domain: a novel DNA binding motif of eukaryotic transcription factors? Cell. 1990;63(3):455-6.

18. Obsil T, Obsilova V. Structural basis for DNA recognition by FOXO proteins. Biochimica et biophysica acta. 2011;1813(11):1946-53.

19. Papanicolaou KN, Izumiya Y, Walsh K. Forkhead transcription factors and cardiovascular biology. Circulation research. 2008;102(1):16-31.

20. Obsil T, Obsilova V. Structure/function relationships underlying regulation of FOXO transcription factors. Oncogene. 2008;27(16):2263-75.

21. Calnan DR, Brunet A. The FoxO code. Oncogene. 2008;27(16):2276-88.

22. Clark KL, Halay ED, Lai E, Burley SK. Co-crystal structure of the HNF-3/fork head DNA-recognition motif resembles histone H5. Nature. 1993;364(6436):412-20.

23. Shen W, Scearce LM, Brestelli JE, Sund NJ, Kaestner KH. Foxa3 (hepatocyte nuclear factor 3gamma) is required for the regulation of hepatic GLUT2 expression and the maintenance of glucose homeostasis during a prolonged fast. The Journal of biological chemistry. 2001;276(46):42812-7.

24. Tsai KL, Sun YJ, Huang CY, Yang JY, Hung MC, Hsiao CD. Crystal structure of the human FOXO3a-DBD/DNA complex suggests the effects of post-translational modification. Nucleic acids research. 2007;35(20):6984-94.

25. Brunet A, Bonni A, Zigmond MJ, Lin MZ, Juo P, Hu LS, Anderson MJ, Arden KC, Blenis J, Greenberg ME. Akt promotes cell survival by phosphorylating and inhibiting a Forkhead transcription factor. Cell. 1999;96(6):857-68.

26. Wang X, Hu S, Liu L. Phosphorylation and acetylation modifications of FOXO3a: Independently or synergistically? Oncology letters. 2017;13(5):2867-72.

27. Tran H, Brunet A, Griffith EC, Greenberg ME. The many forks in FOXO's road. Science's STKE : signal transduction knowledge environment. 2003;2003(172):Re5.

28. Tran H, Brunet A, Grenier JM, Datta SR, Fornace AJ, Jr., DiStefano PS, Chiang LW, Greenberg ME. DNA repair pathway stimulated by the forkhead transcription factor FOXO3a through the Gadd45 protein. Science (New York, NY). 2002;296(5567):530-4.

29. Tzivion G, Dobson M, Ramakrishnan G. FoxO transcription factors; Regulation by AKT and 14-3-3 proteins. Biochimica et biophysica acta. 2011;1813(11):1938-45.

30. Vogt PK, Jiang H, Aoki M. Triple layer control: phosphorylation, acetylation and ubiquitination of FOXO proteins. Cell cycle (Georgetown, Tex). 2005;4(7):908-13.

31. Greer EL, Oskoui PR, Banko MR, Maniar JM, Gygi MP, Gygi SP, Brunet A. The energy sensor AMP-activated protein kinase directly regulates the mammalian FOXO3 transcription factor. The Journal of biological chemistry. 2007;282(41):30107-19.

32. van der Heide LP, Smidt MP. Regulation of FoxO activity by CBP/p300-mediated acetylation. Trends in biochemical sciences. 2005;30(2):81-6.

33. Motta MC, Divecha N, Lemieux M, Kamel C, Chen D, Gu W, Bultsma Y, McBurney M, Guarente L. Mammalian SIRT1 represses forkhead transcription factors. Cell. 2004;116(4):551-63.

34. Brunet A, Sweeney LB, Sturgill JF, Chua KF, Greer PL, Lin Y, Tran H, Ross SE, Mostoslavsky R, Cohen HY, Hu LS, Cheng HL, Jedrychowski MP, Gygi SP, Sinclair DA, Alt FW, Greenberg ME. Stress-dependent regulation of FOXO transcription factors by the SIRT1 deacetylase. Science (New York, NY). 2004;303(5666):2011-5.

35. Hu MC, Lee DF, Xia W, Golfman LS, Ou-Yang F, Yang JY, Zou Y, Bao S, Hanada N, Saso H, Kobayashi R, Hung MC. IkappaB kinase promotes tumorigenesis through inhibition of forkhead FOXO3a. Cell. 2004;117(2):225-37.

36. Karin M, Ben-Neriah Y. Phosphorylation Meets Ubiquitination: The Control of NF-κB Activity. Annual Review of Immunology. 2000;18(1):621-63.

37. Skurk C, Izumiya Y, Maatz H, Razeghi P, Shiojima I, Sandri M, Sato K, Zeng L, Schiekofer S, Pimentel D, Lecker S, Taegtmeyer H, Goldberg AL, Walsh K. The FOXO3a transcription factor regulates cardiac myocyte size downstream of AKT signaling. The Journal of biological chemistry. 2005;280(21):20814-23.

38. Sandri M, Sandri C, Gilbert A, Skurk C, Calabria E, Picard A, Walsh K, Schiaffino S, Lecker SH, Goldberg AL. Foxo transcription factors induce the atrophy-related ubiquitin ligase atrogin-1 and cause skeletal muscle atrophy. Cell. 2004;117(3):399-412.

39. Stitt TN, Drujan D, Clarke BA, Panaro F, Timofeyva Y, Kline WO, Gonzalez M, Yancopoulos GD, Glass DJ. The IGF-1/PI3K/Akt pathway prevents expression of muscle atrophy-induced ubiquitin ligases by inhibiting FOXO transcription factors. Molecular cell. 2004;14(3):395-403.

40. Mouw JK, Ou G, Weaver VM. Extracellular matrix assembly: a multiscale deconstruction. Nature reviews Molecular cell biology. 2014;15(12):771-85.

41. Ricard-Blum S. The collagen family. Cold Spring Harbor perspectives in biology. 2011;3(1):a004978.

42. Macchiarelli G, Ohtani O, Nottola SA, Stallone T, Camboni A, Prado IM, Motta PM. A micro-anatomical model of the distribution of myocardial endomysial collagen. Histology and histopathology. 2002;17(3):699-706.

43. Yu H, Fellows A, Foote K, Yang Z, Figg N, Littlewood T, Bennett M. FOXO3a (Forkhead Transcription Factor O Subfamily Member 3a) Links Vascular Smooth Muscle Cell Apoptosis, Matrix Breakdown, Atherosclerosis, and Vascular Remodeling Through a Novel Pathway Involving MMP13 (Matrix Metalloproteinase 13). Arteriosclerosis, thrombosis, and vascular biology. 2018;38(3):555-65.

44. Zhu JY, Pang ZJ, Yu YH. Regulation of trophoblast invasion: the role of matrix metalloproteinases. Reviews in obstetrics & gynecology. 2012;5(3-4):e137-43.

45. Malemud CJ. Matrix metalloproteinases: role in skeletal development and growth plate disorders. Frontiers in bioscience : a journal and virtual library. 2006;11:1702-15.

46. Reinhard SM, Razak K, Ethell IM. A delicate balance: role of MMP-9 in brain development and pathophysiology of neurodevelopmental disorders. Frontiers in cellular neuroscience. 2015;9:280.

47. Vu TH, Werb Z. Matrix metalloproteinases: effectors of development and normal physiology. Genes & development. 2000;14(17):2123-33.

48. Imai K, Hiramatsu A, Fukushima D, Pierschbacher MD, Okada Y. Degradation of decorin by matrix metalloproteinases: identification of the cleavage sites, kinetic analyses and transforming growth factor-beta1 release. The Biochemical journal. 1997;322 (Pt 3):809-14.

49. Whitelock JM, Murdoch AD, Iozzo RV, Underwood PA. The degradation of human endothelial cell-derived perlecan and release of bound basic fibroblast growth factor by stromelysin, collagenase, plasmin, and heparanases. The Journal of biological chemistry. 1996;271(17):10079-86.

50. Becker-Pauly C, Rose-John S. TNFalpha cleavage beyond TACE/ADAM17: matrix metalloproteinase 13 is a potential therapeutic target in sepsis and colitis. EMBO molecular medicine. 2013;5(7):970-2.

51. Schonbeck U, Mach F, Libby P. Generation of biologically active IL-1 beta by matrix metalloproteinases: a novel caspase-1-independent pathway of IL-1 beta processing. Journal of immunology (Baltimore, Md : 1950). 1998;161(7):3340-6.

52. Fernandez-Patron C, Radomski MW, Davidge ST. Vascular matrix metalloproteinase-2 cleaves big endothelin-1 yielding a novel vasoconstrictor. Circulation research. 1999;85(10):906-11.

53. Diekmann O, Tschesche H. Degradation of kinins, angiotensins and substance P by polymorphonuclear matrix metalloproteinases MMP 8 and MMP 9. Brazilian journal of medical and biological research = Revista brasileira de pesquisas medicas e biologicas. 1994;27(8):1865-76.

54. McQuibban GA, Gong JH, Wong JP, Wallace JL, Clark-Lewis I, Overall CM. Matrix metalloproteinase processing of monocyte chemoattractant proteins generates CC chemokine receptor antagonists with anti-inflammatory properties in vivo. Blood. 2002;100(4):1160-7.

55. Snoek-van Beurden PA, Von den Hoff JW. Zymographic techniques for the analysis of matrix metalloproteinases and their inhibitors. BioTechniques. 2005;38(1):73-83.

56. Etoh T, Inoue H, Yoshikawa Y, Barnard GF, Kitano S, Mori M. Increased expression of collagenase-3 (MMP-13) and MT1-MMP in oesophageal cancer is related to cancer aggressiveness. Gut. 2000;47(1):50-6.

57. Varani J, Hattori Y, Chi Y, Schmidt T, Perone P, Zeigler ME, Fader DJ, Johnson TM. Collagenolytic and gelatinolytic matrix metalloproteinases and their inhibitors in basal cell carcinoma of skin: comparison with normal skin. British journal of cancer. 2000;82(3):657-65.

58. Uria JA, Balbin M, Lopez JM, Alvarez J, Vizoso F, Takigawa M, Lopez-Otin C. Collagenase-3 (MMP-13) expression in chondrosarcoma cells and its regulation by basic fibroblast growth factor. The American journal of pathology. 1998;153(1):91-101.

59. Airola K, Karonen T, Vaalamo M, Lehti K, Lohi J, Kariniemi AL, Keski-Oja J, Saarialho-Kere UK. Expression of collagenases-1 and -3 and their inhibitors TIMP-1 and -3 correlates with the level of invasion in malignant melanomas. British journal of cancer. 1999;80(5-6):733-43.

60. Johansson N, Vaalamo M, Grenman S, Hietanen S, Klemi P, Saarialho-Kere U, Kahari VM. Collagenase-3 (MMP-13) is expressed by tumor cells in invasive vulvar squamous cell carcinomas. The American journal of pathology. 1999;154(2):469-80.

61. Vaalamo M, Karjalainen-Lindsberg ML, Puolakkainen P, Kere J, Saarialho-Kere U. Distinct expression profiles of stromelysin-2 (MMP-10), collagenase-3 (MMP-13), macrophage metalloelastase (MMP-12), and tissue inhibitor of metalloproteinases-3 (TIMP-3) in intestinal ulcerations. The American journal of pathology. 1998;152(4):1005-14.

62. Kozaci LD, Buttle DJ, Hollander AP. Degradation of type II collagen, but not proteoglycan, correlates with matrix metalloproteinase activity in cartilage explant cultures. Arthritis and rheumatism. 1997;40(1):164-74.

63. Stahle-Backdahl M, Sandstedt B, Bruce K, Lindahl A, Jimenez MG, Vega JA, Lopez-Otin C. Collagenase-3 (MMP-13) is expressed during human fetal ossification and re-expressed in postnatal bone remodeling and in rheumatoid arthritis. Laboratory investigation; a journal of technical methods and pathology. 1997;76(5):717-28.

64. Spinale FG, Coker ML, Heung LJ, Bond BR, Gunasinghe HR, Etoh T, Goldberg AT, Zellner JL, Crumbley AJ. A matrix metalloproteinase induction/activation system exists in the human left ventricular myocardium and is upregulated in heart failure. Circulation. 2000;102(16):1944-9.

65. Ries C, Petrides PE. Cytokine regulation of matrix metalloproteinase activity and its regulatory dysfunction in disease. Biological chemistry Hoppe-Seyler. 1995;376(6):345-55.

66. Nagase H. Activation mechanisms of matrix metalloproteinases. Biological chemistry. 1997;378(3-4):151-60.

67. Visse R, Nagase H. Matrix metalloproteinases and tissue inhibitors of metalloproteinases: structure, function, and biochemistry. Circulation research. 2003;92(8):827-39.

68. Borden P, Solymar D, Sucharczuk A, Lindman B, Cannon P, Heller RA. Cytokine control of interstitial collagenase and collagenase-3 gene expression in human chondrocytes. The Journal of biological chemistry. 1996;271(38):23577-81.

69. Mengshol JA, Vincenti MP, Coon CI, Barchowsky A, Brinckerhoff CE. Interleukin-1 induction of collagenase 3 (matrix metalloproteinase 13) gene expression in chondrocytes requires p38, c-Jun N-terminal kinase, and nuclear factor kappaB: differential regulation of collagenase 1 and collagenase 3. Arthritis and rheumatism. 2000;43(4):801-11.

70. Rosenkranz S. TGF-beta1 and angiotensin networking in cardiac remodeling. Cardiovascular research. 2004;63(3):423-32.

71. Liberati NT, Datto MB, Frederick JP, Shen X, Wong C, Rougier-Chapman EM, Wang XF. Smads bind directly to the Jun family of AP-1 transcription factors. Proceedings of the National Academy of Sciences of the United States of America. 1999;96(9):4844-9.

72. Yuan W, Varga J. Transforming growth factor-beta repression of matrix metalloproteinase-1 in dermal fibroblasts involves Smad3. The Journal of biological chemistry. 2001;276(42):38502-10.

73. Czuwara-Ladykowska J, Sementchenko VI, Watson DK, Trojanowska M. Ets1 is an effector of the transforming growth factor beta (TGF-beta) signaling pathway and an antagonist of the profibrotic effects of TGF-beta. The Journal of biological chemistry. 2002;277(23):20399-408.

74. Hall MC, Young DA, Waters JG, Rowan AD, Chantry A, Edwards DR, Clark IM. The comparative role of activator protein 1 and Smad factors in the regulation of Timp-1 and MMP-1 gene expression by transforming growth factor-beta 1. The Journal of biological chemistry. 2003;278(12):10304-13.

75. Uria JA, Jimenez MG, Balbin M, Freije JM, Lopez-Otin C. Differential effects of transforming growth factor-beta on the expression of collagenase-1 and collagenase-3 in human fibroblasts. The Journal of biological chemistry. 1998;273(16):9769-77.

76. Han YP, Tuan TL, Hughes M, Wu H, Garner WL. Transforming growth factor-beta - and tumor necrosis factor-alpha -mediated induction and proteolytic activation of MMP-9 in human skin. The Journal of biological chemistry. 2001;276(25):22341-50.

77. Boixel C, Fontaine V, Rucker-Martin C, Milliez P, Louedec L, Michel JB, Jacob MP, Hatem SN. Fibrosis of the left atria during progression of heart failure is associated with increased matrix metalloproteinases in the rat. Journal of the American College of Cardiology. 2003;42(2):336-44.

78. Prescott MF, Sawyer WK, Von Linden-Reed J, Jeune M, Chou M, Caplan SL, Jeng AY. Effect of matrix metalloproteinase inhibition on progression of atherosclerosis and aneurysm in LDL receptor-deficient mice overexpressing MMP-3, MMP-12, and MMP-13 and on restenosis in rats after balloon injury. Ann N Y Acad Sci. 1999;878:179-90.

79. Sukhova GK, Schonbeck U, Rabkin E, Schoen FJ, Poole AR, Billinghurst RC, Libby P. Evidence for increased collagenolysis by interstitial collagenases-1 and -3 in vulnerable human atheromatous plaques. Circulation. 1999;99(19):2503-9.

80. Becher PM, Gotzhein F, Klingel K, Escher F, Blankenberg S, Westermann D, Lindner D. Cardiac Function Remains Impaired Despite Reversible Cardiac Remodeling after Acute Experimental Viral Myocarditis. J Immunol Res. 2017;2017:6590609.

81. Gunja-Smith Z, Morales AR, Romanelli R, Woessner JF, Jr. Remodeling of human myocardial collagen in idiopathic dilated cardiomyopathy. Role of metalloproteinases and pyridinoline cross-links. The American journal of pathology. 1996;148(5):1639-48.

82. Spinale FG, Coker ML, Thomas CV, Walker JD, Mukherjee R, Hebbar L. Time-dependent changes in matrix metalloproteinase activity and expression during the progression of congestive heart failure: relation to ventricular and myocyte function. Circulation research. 1998;82(4):482-95.

83. Spinale FG, Coker ML, Krombach SR, Mukherjee R, Hallak H, Houck WV, Clair MJ, Kribbs SB, Johnson LL, Peterson JT, Zile MR. Matrix metalloproteinase inhibition

during the development of congestive heart failure : effects on left ventricular dimensions and function. Circulation research. 1999;85(4):364-76.

84. Klotz S, Foronjy RF, Dickstein ML, Gu A, Garrelds IM, Danser AH, Oz MC, D'Armiento J, Burkhoff D. Mechanical unloading during left ventricular assist device support increases left ventricular collagen cross-linking and myocardial stiffness. Circulation. 2005;112(3):364-74.

85. Thomas CV, Coker ML, Zellner JL, Handy JR, Crumbley AJ, 3rd, Spinale FG. Increased matrix metalloproteinase activity and selective upregulation in LV myocardium from patients with end-stage dilated cardiomyopathy. Circulation. 1998;97(17):1708-15.

86. Nian M, Lee P, Khaper N, Liu P. Inflammatory cytokines and postmyocardial infarction remodeling. Circulation research. 2004;94(12):1543-53.

87. Scholz H, Aukrust P, Damas JK, Tonstad S, Sagen EL, Kolset SO, Hall C, Yndestad A, Halvorsen B. 8-isoprostane increases scavenger receptor A and matrix metalloproteinase activity in THP-1 macrophages, resulting in long-lived foam cells. European journal of clinical investigation. 2004;34(7):451-8.

88. Siwik DA, Colucci WS. Regulation of matrix metalloproteinases by cytokines and reactive oxygen/nitrogen species in the myocardium. Heart failure reviews. 2004;9(1):43-51.

89. Siwik DA, Pagano PJ, Colucci WS. Oxidative stress regulates collagen synthesis and matrix metalloproteinase activity in cardiac fibroblasts. American journal of physiology Cell physiology. 2001;280(1):C53-60.

90. Wainwright CL. Matrix metalloproteinases, oxidative stress and the acute response to acute myocardial ischaemia and reperfusion. Current opinion in pharmacology. 2004;4(2):132-8.

91. Lin TC, Li CY, Tsai CS, Ku CH, Wu CT, Wong CS, Ho ST. Neutrophil-mediated secretion and activation of matrix metalloproteinase-9 during cardiac surgery with cardiopulmonary bypass. Anesthesia and analgesia. 2005;100(6):1554-60.

92. Mayers I, Hurst T, Puttagunta L, Radomski A, Mycyk T, Sawicki G, Johnson D, Radomski MW. Cardiac surgery increases the activity of matrix metalloproteinases and nitric oxide synthase in human hearts. The Journal of thoracic and cardiovascular surgery. 2001;122(4):746-52.

93. Mayers I, Hurst T, Radomski A, Johnson D, Fricker S, Bridger G, Cameron B, Darkes M, Radomski MW. Increased matrix metalloproteinase activity after canine cardiopulmonary bypass is suppressed by a nitric oxide scavenger. The Journal of thoracic and cardiovascular surgery. 2003;125(3):661-8.

94. Fu X, Kao JL, Bergt C, Kassim SY, Huq NP, d'Avignon A, Parks WC, Mecham RP, Heinecke JW. Oxidative cross-linking of tryptophan to glycine restrains matrix metalloproteinase activity: specific structural motifs control protein oxidation. The Journal of biological chemistry. 2004;279(8):6209-12.

95. Fu X, Kassim SY, Parks WC, Heinecke JW. Hypochlorous acid oxygenates the cysteine switch domain of pro-matrilysin (MMP-7). A mechanism for matrix metalloproteinase activation and atherosclerotic plaque rupture by myeloperoxidase. The Journal of biological chemistry. 2001;276(44):41279-87.

96. Lee HY, Chung JW, Youn SW, Kim JY, Park KW, Koo BK, Oh BH, Park YB, Chaqour B, Walsh K, Kim HS. Forkhead transcription factor FOXO3a is a negative regulator of angiogenic immediate early gene CYR61, leading to inhibition of vascular smooth muscle cell proliferation and neointimal hyperplasia. Circulation research. 2007;100(3):372-80.

97. Chen CC, Mo FE, Lau LF. The angiogenic factor Cyr61 activates a genetic program for wound healing in human skin fibroblasts. The Journal of biological chemistry. 2001;276(50):47329-37.

98. Castrillon DH, Miao L, Kollipara R, Horner JW, DePinho RA. Suppression of ovarian follicle activation in mice by the transcription factor Foxo3a. Science (New York, NY). 2003;301(5630):215-8.

99. Skurk C, Maatz H, Kim HS, Yang J, Abid MR, Aird WC, Walsh K. The Akt-regulated forkhead transcription factor FOXO3a controls endothelial cell viability through modulation of the caspase-8 inhibitor FLIP. The Journal of biological chemistry. 2004;279(2):1513-25.

100. Klump WM, Bergmann I, Muller BC, Ameis D, Kandolf R. Complete nucleotide sequence of infectious Coxsackievirus B3 cDNA: two initial 5' uridine residues are regained during plus-strand RNA synthesis. J Virol. 1990;64(4):1573-83.

101. Yanagawa B, Spiller OB, Proctor DG, Choy J, Luo H, Zhang HM, Suarez A, Yang D, McManus BM. Soluble recombinant coxsackievirus and adenovirus receptor abrogates coxsackievirus b3-mediated pancreatitis and myocarditis in mice. J Infect Dis. 2004;189(8):1431-9.

102. Lutgens E, Daemen MJ, de Muinck ED, Debets J, Leenders P, Smits JF. Chronic myocardial infarction in the mouse: cardiac structural and functional changes. Cardiovascular research. 1999;41(3):586-93.

103. Jenke A, Holzhauser L, Lobel M, Savvatis K, Wilk S, Weithauser A, Pinkert S, Tschope C, Klingel K, Poller W, Scheibenbogen C, Schultheiss HP, Skurk C. Adiponectin promotes coxsackievirus B3 myocarditis by suppression of acute anti-viral immune responses. Basic Res Cardiol. 2014;109(3):408.

104. Klingel K, Hohenadl C, Canu A, Albrecht M, Seemann M, Mall G, Kandolf R. Ongoing enterovirus-induced myocarditis is associated with persistent heart muscle infection: quantitative analysis of virus replication, tissue damage, and inflammation. Proceedings of the National Academy of Sciences of the United States of America. 1992;89(1):314-8.

105. Webb AE, Brunet A. FOXO transcription factors: key regulators of cellular quality control. Trends in biochemical sciences. 2014;39(4):159-69.

106. Ni YG, Berenji K, Wang N, Oh M, Sachan N, Dey A, Cheng J, Lu G, Morris DJ, Castrillon DH, Gerard RD, Rothermel BA, Hill JA. Foxo transcription factors blunt cardiac hypertrophy by inhibiting calcineurin signaling. Circulation. 2006;114(11):1159-68.

107. Galasso G, De Rosa R, Piscione F, Iaccarino G, Vosa C, Sorriento D, Piccolo R, Rapacciuolo A, Walsh K, Chiariello M. Myocardial expression of FOXO3a-Atrogin-1 pathway in human heart failure. European journal of heart failure. 2010;12(12):1290-6.

108. Loebel M, Holzhauser L, Hartwig JA, Shukla PC, Savvatis K, Jenke A, Gast M, Escher F, Becker SC, Bauer S, Stroux A, Beling A, Kespohl M, Pinkert S, Fechner H, Kuehl U, Lassner D, Poller W, Schultheiss HP, Zeller T, Blankenberg S, Papageorgiou AP, Heymans S, Landmesser U, Scheibenbogen C, Skurk C. The forkhead transcription factor Foxo3 negatively regulates natural killer cell function and viral clearance in myocarditis. European heart journal. 2018;39(10):876-87.

109. Kops GJ, Dansen TB, Polderman PE, Saarloos I, Wirtz KW, Coffer PJ, Huang TT, Bos JL, Medema RH, Burgering BM. Forkhead transcription factor FOXO3a protects quiescent cells from oxidative stress. Nature. 2002;419(6904):316-21.

110. Nemoto S, Finkel T. Redox regulation of forkhead proteins through a p66shc-dependent signaling pathway. Science (New York, NY). 2002;295(5564):2450-2.

111. Sundaresan NR, Gupta M, Kim G, Rajamohan SB, Isbatan A, Gupta MP. Sirt3 blocks the cardiac hypertrophic response by augmenting Foxo3a-dependent antioxidant defense mechanisms in mice. The Journal of clinical investigation. 2009;119(9):2758-71.

112. Tan WQ, Wang K, Lv DY, Li PF. Foxo3a inhibits cardiomyocyte hypertrophy through transactivating catalase. The Journal of biological chemistry. 2008;283(44):29730-9.

113. Lee HY, You HJ, Won JY, Youn SW, Cho HJ, Park KW, Park WY, Seo JS, Park YB, Walsh K, Oh BH, Kim HS. Forkhead factor, FOXO3a, induces apoptosis of endothelial cells through activation of matrix metalloproteinases. Arteriosclerosis, thrombosis, and vascular biology. 2008;28(2):302-8.

114. Potente M, Urbich C, Sasaki K, Hofmann WK, Heeschen C, Aicher A, Kollipara R, DePinho RA, Zeiher AM, Dimmeler S. Involvement of Foxo transcription factors in

angiogenesis and postnatal neovascularization. The Journal of clinical investigation. 2005;115(9):2382-92.

115. Morita N, Mandel WJ, Kobayashi Y, Karagueuzian HS. Cardiac fibrosis as a determinant of ventricular tachyarrhythmias. Journal of arrhythmia. 2014;30(6):389-94.

116. Shiojima I, Sato K, Izumiya Y, Schiekofer S, Ito M, Liao R, Colucci WS, Walsh K. Disruption of coordinated cardiac hypertrophy and angiogenesis contributes to the transition to heart failure. The Journal of clinical investigation. 2005;115(8):2108-18.

117. Pramod S, Shivakumar K. Mechanisms in cardiac fibroblast growth: an obligate role for Skp2 and FOXO3a in ERK1/2 MAPK-dependent regulation of p27kip1. American journal of physiology Heart and circulatory physiology. 2014;306(6):H844-55.

118. Xin Z, Ma Z, Hu W, Jiang S, Yang Z, Li T, Chen F, Jia G, Yang Y. FOXO1/3: Potential suppressors of fibrosis. Ageing research reviews. 2018;41:42-52.

119. Pei XM, Yung BY, Yip SP, Chan LW, Wong CS, Ying M, Siu PM. Protective effects of desacyl ghrelin on diabetic cardiomyopathy. Acta Diabetol. 2015;52(2):293-306.

120. Whittaker M, Floyd CD, Brown P, Gearing AJ. Design and therapeutic application of matrix metalloproteinase inhibitors. Chem Rev. 1999;99(9):2735-76.

121. Herzog E, Gu A, Kohmoto T, Burkhoff D, Hochman JS. Early Activation of Metalloproteinases after Experimental Myocardial Infarction Occurs in Infarct and Non-infarct Zones. Cardiovasc Pathol. 1998;7(6):307-12.

122. Romanic AM, Burns-Kurtis CL, Gout B, Berrebi-Bertrand I, Ohlstein EH. Matrix metalloproteinase expression in cardiac myocytes following myocardial infarction in the rabbit. Life Sci. 2001;68(7):799-814.

123. Sawicki G, Menon V, Jugdutt BI. Improved balance between TIMP-3 and MMP-9 after regional myocardial ischemia-reperfusion during AT1 receptor blockade. J Card Fail. 2004;10(5):442-9.

124. Lindsey ML, Zamilpa R. Temporal and spatial expression of matrix metalloproteinases and tissue inhibitors of metalloproteinases following myocardial infarction. Cardiovasc Ther. 2012;30(1):31-41.

125. Norambuena-Soto I, Nunez-Soto C, Sanhueza-Olivares F, Cancino-Arenas N, Mondaca-Ruff D, Vivar R, Diaz-Araya G, Mellado R, Chiong M. Transforming growth factor-beta and Forkhead box O transcription factors as cardiac fibroblast regulators. Bioscience trends. 2017;11(2):154-62.

126. Yoon HE, Kim SJ, Kim SJ, Chung S, Shin SJ. Tempol attenuates renal fibrosis in mice with unilateral ureteral obstruction: the role of PI3K-Akt-FoxO3a signaling. Journal of Korean medical science. 2014;29(2):230-7.

127. Ahmed SH, Clark LL, Pennington WR, Webb CS, Bonnema DD, Leonardi AH, McClure CD, Spinale FG, Zile MR. Matrix Metalloproteinases/Tissue Inhibitors of Metalloproteinases. Circulation. 2006;113(17):2089-96.

Statutory Declaration

“I, Xheni Voloti, by personally signing this document in lieu of an oath, hereby affirm that I prepared the submitted dissertation on the topic “FOXO3a and cardiac matrix remodeling-Regulation of MMP-13 expression” (“FOXO3a und das kardiale Remodeling der extrazellulären Matrix -Regulation der MMP-13 Expression”), independently and without the support of third parties, and that I used no other sources and aids than those stated.
All parts which are based on the publications or presentations of other authors, either in letter or in spirit, are specified as such in accordance with the citing guidelines. The sections on methodology (in particular regarding practical work, laboratory regulations, statistical processing) and results (in particular regarding figures, charts and tables) are exclusively my responsibility.

I declare that I have not yet submitted this dissertation in identical or similar form to another Faculty.

The significance of this statutory declaration and the consequences of a false statutory declaration under criminal law (Sections 156, 161 of the German Criminal Code) are known to me.”

Date Signature

My curriculum vitae does not appear in the electronic version of my paper for reasons of data protection.

Acknowledgements

I will forever be grateful to my supervisor Prof. Dr. med. Carsten Skurk for believing in me, supporting me since the beginning and giving me the opportunity to do research. I thank him for his guidance and patience throughout the entire process and for continuously reflecting passion and love for scientific research.

Finally, but most importantly, I would like to thank my family, for this work would have never been possible without their continuous support. I thank my parents for the love and strength they still continue to give me. Thank you for always and undoubtedly believing in me. I thank my brother for his love, humor and positive attitude.